

# Towards mechanistic understanding of mechanochemical reactions using real-time *in situ* monitoring

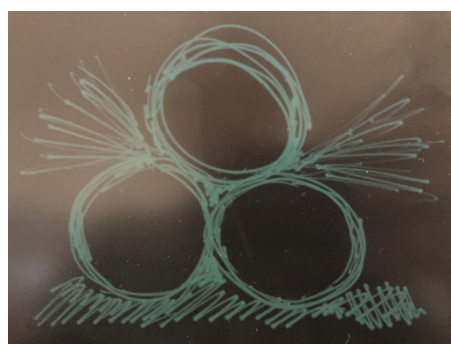
Stipe Lukin,<sup>a</sup> Luzia S. Germann,<sup>b</sup> Tomislav Friščić,<sup>b,\*</sup> Ivan Halasz,<sup>a,\*</sup>

a) Ruđer Bošković Institute, Bijenička c. 54, 10000 Zagreb, Croatia; b) Department of Chemistry, McGill University, 801 Sherbrooke St. W. H3A 0B8 Montreal, Canada

Email: [tomislav.friscic@mcgill.ca](mailto:tomislav.friscic@mcgill.ca); [ivan.halasz@irb.hr](mailto:ivan.halasz@irb.hr)

## CONSPECTUS

The past two decades have witnessed a rapid emergence of interest in mechanochemistry – chemical and materials reactivity achieved or sustained by the action of mechanical force – which has led to a rapid growth of application of mechanochemistry to almost all areas of modern chemical and materials synthesis: from organic, inorganic and organometallic chemistry to enzymatic reactions, formation of metal-organic frameworks, hybrid perovskites and nanoparticle-based materials. The recent success of mechanochemistry by ball milling has also raised questions on the underlying mechanisms, and has led to the realization that the rational development and effective harnessing of mechanochemical reactivity for cleaner and more efficient chemical manufacturing will critically depend on establishing a mechanistic understanding of these reactions. Despite their long history, the development of such a knowledge framework for mechanochemical reactions is still incomplete. This is in part due to the, until recently, unsurmountable challenge of directly observing transformations taking place in a rapidly oscillating or rotating milling vessel, with the sample being under the continuous impact of milling media. A transformative change in mechanistic studies of milling reactions was recently introduced through the first two methodologies for real-time *in situ* monitoring based on synchrotron powder X-ray diffraction and Raman spectroscopy. Introduced in 2013 and 2014, the two new techniques have inspired a period of tremendous method development, resulting also in new techniques for mechanistic mechanochemical studies that are based on temperature and/or pressure monitoring, extended X-ray fine structure (EXAFS) and latest, nuclear magnetic resonance (NMR) spectroscopy. The new technologies available for real-time monitoring have now inspired the development of experimental strategies and advanced data analysis approaches for the identification and quantification of short-lived reaction intermediates, the development of new mechanistic models, as well as the emergence of more complex monitoring methodologies based on two or three simultaneous monitoring approaches. The use of these new opportunities has, in less than a decade, enabled the first real-time observations of mechanochemical reaction kinetics, and the first studies of how the presence of additives, or other means of modifying the mechanochemical reaction, influence reaction rates and pathways. These studies have revealed multi-step reaction mechanisms, enabled the identification of autocatalysis, as well as identified molecules and materials that have previously not been known or have even been considered not possible to synthesize through conventional approaches. Mechanistic studies through *in situ*



powder X-ray diffraction (PXRD) and Raman spectroscopy have highlighted the formation of supramolecular complexes (for example, cocrystals) as critical intermediates in organic and metal-organic synthesis, and have also been combined with isotope labelling strategies to provide a deeper insight into mechanochemical reaction mechanisms and atomic and molecular dynamics under milling conditions. This *Account* provides an overview of this exciting, rapidly evolving field by presenting the development and concepts behind the new methodologies for real-time *in situ* monitoring of mechanochemical reactions, outlining key advances in mechanistic understanding of mechanochemistry, and presenting selected studies important for pushing forward the boundaries of measurement techniques, data analysis and mapping of reaction mechanisms.

## KEY REFERENCES

- Frišćić, T.; Halasz, I.; Beldon, P. J.; Belenguer, A. M.; Adams, F.; Kimber, S. A. J.; Honkimäki, V.; Dinnebier, R. E. Real-Time and *in Situ* Monitoring of Mechanochemical Milling Reactions. *Nat. Chem.* **2013**, *5*, 66–73.<sup>1</sup> *The first implementation of an in situ technique that was based on synchrotron powder X-ray diffraction and enabled the monitoring of the evolution of crystalline substances.*
- Gracin, D.; Štrukil, V.; Frišćić, T.; Halasz, I.; Užarević, K. Laboratory Real-Time and *in Situ* Monitoring of Mechanochemical Milling Reactions by Raman Spectroscopy. *Angew. Chem. Int. Ed.* **2014**, *53*, 6193–6197.<sup>2</sup> *The first implementation of Raman spectroscopy for in situ monitoring of mechanochemical reactions, as an accessible laboratory technique applicable to a broad range of materials.*
- Lukin, S.; Tireli, M.; Stolar, T.; Barišić, D.; Blanco, M. V.; Di Michiel, M.; Užarević, K.; Halasz, I. Isotope Labeling Reveals Fast Atomic and Molecular Exchange in Mechanochemical Milling Reactions. *J. Am. Chem. Soc.* **2019**, *141*, 1212–1216.<sup>3</sup> *Observation of inherent atomic and molecular exchange between milled particles demonstrating how slow solid-state diffusion is overcome by milling.*
- Germann, L. S.; Arhangelskis, M.; Etter, M.; Dinnebier, R. E.; Frišćić, T. Challenging the Ostwald Rule of Stages in Mechanochemical Cocrystallisation. *Chem. Sci.* **2020**, *11*, 10092–10100.<sup>4</sup> *Demonstration of how the variation in the design and material of the mechanochemical experiment can enable the modification of reaction profiles to obtain thermodynamically stable or metastable products.*

## INTRODUCTION

A major contribution to the recent acceptance of mechanochemistry by the broader research community is the introduction of the very first methodologies for direct, *in situ* real-time observation of the underlying structural and chemical changes. Our team facilitated the development of such techniques in 2013<sup>1</sup> and 2014<sup>2</sup> by demonstrating the possibility to use synchrotron X-ray diffraction and Raman spectroscopy, respectively, to follow ball milling transformations in real time, and in that way obtain previously inaccessible details of the profiles and kinetics of ball milling mechanochemical reactions, with consequences for understanding the underlying thermodynamics.<sup>3,4</sup>

Over the past two decades, ball milling has become a versatile solventless synthesis technique with applications in a wide range of areas, from organic, inorganic and coordination chemistry, to the synthesis of functional materials, nanoparticle-based systems, as well as pharmaceutical cocrystals and polymorphs.<sup>5,6</sup> Milling, traditionally seen as a solids processing tool, is also the foundation of a wide range of mechanochemical processes, including organocatalytic, metal-, as well as enzyme-catalyzed reactions, in which chemical and materials transformations are facilitated through diverse additives. Simplicity of mechanosynthesis and its compliance with principles of “Green chemistry”<sup>7</sup> highlights potential for sustainable manufacturing, as evident by its inclusion among the top ten technologies that can change the world by the International Union for Pure and Applied Chemistry (IUPAC).<sup>8</sup>

Following the course of mechanochemical transformations has previously relied on temperature and pressure monitoring, or a step-by-step approach which, although highly informative, is more laborious and is affected by changes in temperature and exposure to atmosphere.<sup>9</sup> The outcomes of step-by-step monitoring can thus be misleading,<sup>10,11</sup> and fine details of ball milling chemistry at reaction times under a minute often cannot be addressed reliably.<sup>12</sup> *In situ* monitoring provides a reliable and immediate overview of reactivity in a milling process without interrupting it.<sup>13,14</sup> The importance of *in situ* monitoring is evident from the rapid development and transfer of methodology to new laboratories and synchrotron beamlines. For example, following the initial development at the ESRF – The European synchrotron (Grenoble, France),<sup>1,15</sup> methods for *in situ* monitoring of mechanochemical reactions by powder X-ray diffraction (PXRD) are now implemented at five synchrotron centers. Both DESY (Hamburg, Germany) and ESRF provide dedicated beamline setups for real-time monitoring of mechanochemistry in shaker mills. An innovative and unconventional setup developed at PSI (Villigen, Switzerland) provides unmatched signal-to-noise ratio and clear peak profiles.<sup>16</sup> The BESSY II facility (Berlin, Germany) provides an optimized setup for *in situ* monitoring using a vertically vibrating ball mill,<sup>17</sup> while *in situ* monitoring is also since recently available at the Diamond synchrotron (Chilton, UK).

Here, we provide an overview of recent contributions to the development of methods for real-time and *in situ* monitoring of mechanochemical reaction kinetics, mechanisms and thermodynamics, focusing mostly on our work, but also providing a broader context of understanding and designing mechanochemical reactivity.

## METHODOLOGY

The most popular devices for mechanochemical synthesis by ball milling appear to be shaker (mixer) mills, with reactions performed in closed, rapidly oscillating jars that can be made from a variety of materials – from stainless steel or other metals, to various ceramics and plastics. All these materials are, in principle, compatible with real-time reaction monitoring. For real-time Raman spectroscopy monitoring the choice of the milling jar material is limited to optically transparent solids, such as different types of plastics or inorganic materials (*e.g.*, quartz,<sup>18</sup> sapphire<sup>19</sup>). Although recent work has highlighted routes to follow mechanochemical reactions using chemoluminescence<sup>20</sup> and magnetic resonance techniques,<sup>21</sup> the only currently well-established techniques are based on Raman spectroscopy and synchrotron PXRD.

### **Powder X-Ray Diffraction monitoring**

Unless a specialized mill<sup>16</sup> or thin-walled jars are used,<sup>17</sup> *in situ* X-ray diffraction on a sample in a rapidly oscillating reaction vessel requires a synchrotron X-ray beam of intensity and photon energy sufficiently high to penetrate the vessel walls.<sup>22</sup> In the most basic setup, the X-ray beam is passed through the bottom part of the inner chamber of the reaction vessel, which is oscillating perpendicular to the beam (Figure 1). The vessel is most commonly made from X-ray-amorphous and low-absorbing plastic, such as poly (methyl metacrylate) (PMMA), but also other materials, including crystalline ones such as steel and aluminum, can also be used. Using a 2-dimensional (2D) detector, the entire diffraction pattern is collected at once, enabling data collection with time resolution in seconds.

### **Raman spectroscopy monitoring**

Another technique capable of probing the reaction mixture composition *in situ* and with time resolution in seconds is Raman spectroscopy.<sup>2,23</sup> Here, the optical transparency of PMMA, sapphire,<sup>19</sup> or other types of vessels allows penetration of the laser beam inside the reaction vessel to interact with the sample (Figure 1b). The laser beam is guided by a fiber optics probe to enter the reaction vessel from below and also collect the Raman scattering signal. While the use of PXRD is limited to a synchrotron X-ray source, *in situ* Raman spectroscopy is readily implemented in a laboratory using a wide range of portable and affordable Raman spectroscopy setups.

### **Tandem monitoring**

The two *in situ* monitoring approaches are complementary, with PXRD primarily suited to detect bulk crystalline species, and Raman spectroscopy providing a signal from the entire sample. The two types of measurements are mutually independent, allowing the combination into a single experimental setup.<sup>24,25</sup> Such tandem approach, also in combination with temperature or pressure measurement, was successfully applied on a variety of chemical systems in the last several years.<sup>26–28</sup> Recently, tandem monitoring by combining synchrotron X-ray diffraction with extended X-ray fine structure spectroscopy (EXAFS) was also demonstrated.<sup>29</sup>

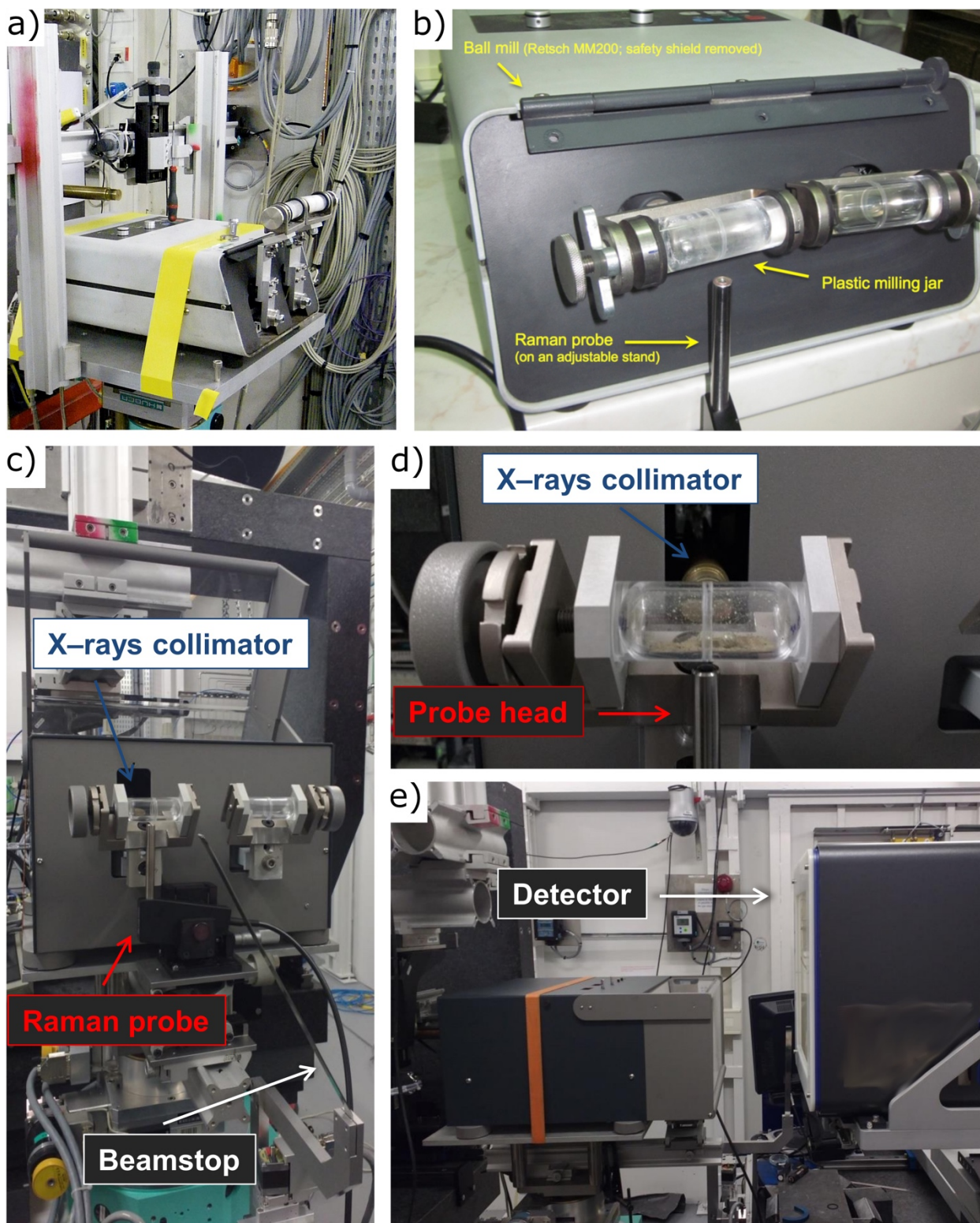


**Figure 1.** The first setups for *in situ* monitoring using (a) powder X-ray diffraction, (b) Raman spectroscopy. (c) A setup with a remotely controlled mill for tandem monitoring. The holding hands of the mill are at an angle of  $45^\circ$  to allow simultaneous approach of the X-ray beam and the laser light to the jar. (d) Close-up on the reaction jar with the collimator and the Raman probe

positioned at the same portion of the sample. (e) Side view of the mill and the detector. For conventional PXRD monitoring, the detector is moved further away.

### Temperature monitoring

Monitoring the temperature of the reaction mixture is probably among the oldest approaches for indirect monitoring of milling mechanochemistry, typically achieved through thermocouples placed onto, or embedded within, the milling jar walls.<sup>30</sup> In general, this is a low-sensitivity technique, mostly applicable to highly exothermic processes and mechanically-induced self-sustained reactions (MSRs),<sup>31</sup> and was recently simplified through the use of infrared thermal monitoring.<sup>26</sup> Superior precision and almost direct detection of sample temperature were recently demonstrated by placing a sensor in the immediate vicinity of the internal surface of the milling vessel, which revealed that heat generation in the course of mechanochemical reactions such as metal-organic framework (MOF) formation comes mostly from friction, rather than reaction enthalpy (Figure 2).<sup>28</sup>

### Pressure monitoring

Another long-known approach for monitoring mechanochemical reaction progress is by measuring pressure changes within the sealed milling vessel,<sup>32,33</sup> which provides information on the absorption, release or, in case of an exothermic process,<sup>34</sup> thermal expansion of a gas. The use of pressure as a handle for monitoring reaction progress provided early examples of multi-step mechanochemical processes in the context of inorganic chemistry,<sup>35</sup> but stipulates the participation of gaseous reactants or products.<sup>36</sup> Our team recently demonstrated how using a carbonate reactant permits direct monitoring of the mechanochemical synthesis of MOFs through pressure increase resulting from CO<sub>2</sub> release (Figure 2).<sup>37</sup>

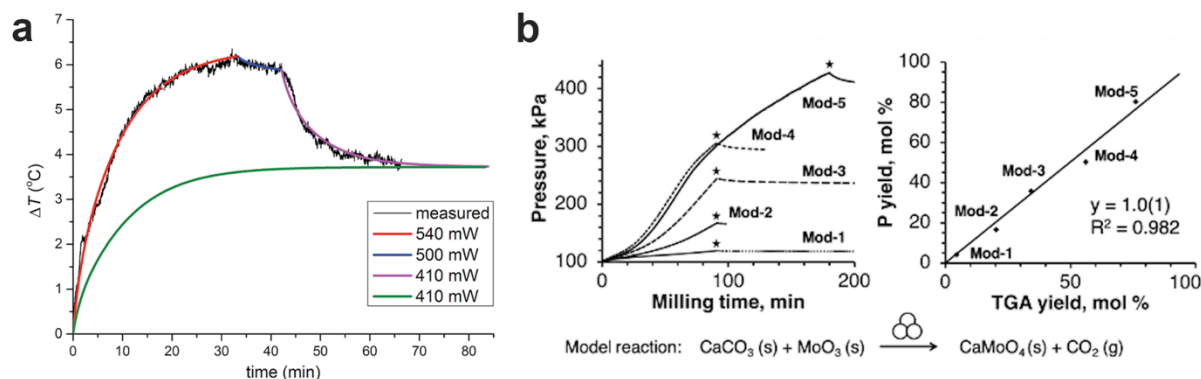
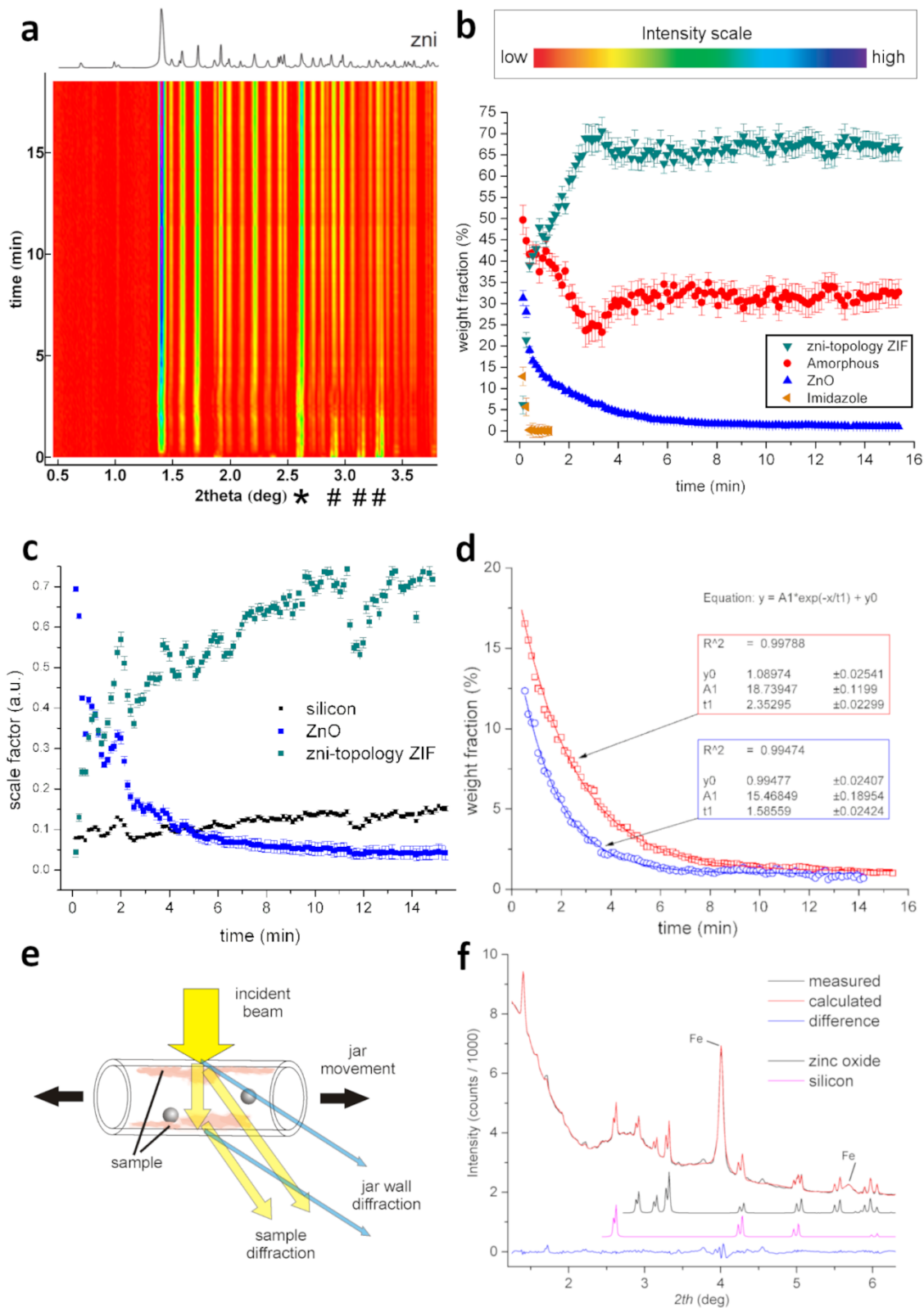


Figure 2. Temperature and pressure in situ monitoring. (a) Numerical modeling of heat flow demonstrating the dominant contribution from friction and (b) pressure-yield correlates with thermogravimetry-determined yield. Reproduced with permission from references 28 and 37. Copyright

### Data processing

The *in situ* collected X-ray diffraction data are usually of sufficient quality for quantitative or qualitative analysis. Simple visual analysis of two-dimensional background-corrected diffractograms (Figure 3a) can reveal a plethora of information, such as the number of

transformations occurring during milling and even preliminary identification of participating phases. If crystal structures of all participating phases are known, quantitative analysis of reaction profiles is accessible through a Rietveld refinement.<sup>38</sup> Otherwise, qualitative reaction profiles can be extracted by a Pawley refinement<sup>39</sup> or single-peak fitting.<sup>1</sup> The inclusion of an X-ray scattering standard, such as crystalline silicon, permits estimating homogeneity of the reaction mixture, quantification of the amorphous content, as well as determination of the instrument contribution to peak width and shape and thus to information such as average particle strain and size (Figure 3).<sup>40,41</sup>



**Figure 3.** The use of crystalline silicon as an internal scattering standard enables quantitative analysis of the milled reaction mixture and an assessment of amorphous content *in situ*: (a) mechanochemical formation of Zn(Im)<sub>2</sub> framework by liquid-assisted grinding and (b) Rietveld-

extracted weight fractions. Silicon reflection marked with '\*'. (c) variations of the scale factor mark redistribution of the milled material in the jar and are scaled by the silicon internal standard giving rise to (d) smooth curves that can be used for kinetic modeling. (e) Diffraction from two parts of the sample residing on opposite sides of the jar causing double diffraction that (f) can be modeled with a shift in diffraction maxima proportional to  $\tan(2\theta)$ . Adapted with permission from ref. 1 (copyright 2012 Nature Publishing Group) and ref. 40 (copyright 2014 Royal Society of Chemistry). Data from ref. 40 in e).

For monitoring by Raman spectroscopy, a time-resolved 2D plot can again serve to obtain a qualitative description of the reaction, while several possible approaches to deduce the reaction profiles. While a qualitative reaction profile is accessible by extracting intensities of characteristic Raman bands,<sup>42</sup> a quantitative assessment is also possible employing a multivariate analysis such as least-squares regression if corresponding reference Raman spectra for each of the participating species are collected. Such a quantitative approach remains applicable also when a Rietveld refinement is not possible,<sup>25</sup> while a qualitative profile could also be obtained without reference spectra using factor analysis such as multivariate curve resolution.<sup>43</sup> In general, temperature and pressure monitoring will require a combination with at least one of the spectroscopic or diffraction *in situ* methods to allow a correlation with changes in physical and chemical properties.<sup>27</sup>

## SCOPE

Techniques for *in situ* monitoring of mechanochemical reactions have now been applied to a wide range of compounds and materials. In many cases, such monitoring revealed multi-step sequences, including short-lived intermediates not observed in corresponding solvent-based environments. *In situ* monitoring provides also the long-lacking foundation for quantitative studies of catalytic and autocatalytic effects of milling additives. However, we note that additives, as well as any metastable or short-lived intermediates, will usually be present in small amounts, which brings into focus limits of detectability. These limits are still poor for temperature and pressure monitoring, and are difficult to generalize for reaction monitoring using PXRD and Raman techniques. In the case of PXRD-based monitoring, the detection limits will depend on the crystallinity, as well as the scattering power of the individual mixture components, which may be accounted for by choosing a different X-ray wavelength. In spectroscopic monitoring by Raman spectroscopy, the strength of the signal will depend on the Raman cross-section, which may differ significantly across diverse molecular species and materials, and will also be dependent on the wavelength of the incident laser beam. A general overview of advantages and limitations of different *in situ* monitoring techniques is provided in Table 1.

Table 1. Overview of advantages and limitations of the most common techniques for *in situ* monitoring of mechanochemical ball milling reactions.

	Advantages	Limitations	Type of material

General	<ul style="list-style-type: none"> <li>○ allows uninterrupted monitoring</li> <li>○ time-resolved information with time resolution in seconds or less</li> <li>○ fast and reliable</li> </ul>	<ul style="list-style-type: none"> <li>○ may suffer from poor mixing or if the milled material gets cluttered</li> <li>○ may be challenging to detect phases that appear in small amounts</li> <li>○ lower data quality in comparison to dedicated ex situ analysis approaches</li> </ul>	<ul style="list-style-type: none"> <li>○ any</li> </ul>
PXRD	<ul style="list-style-type: none"> <li>○ direct identification of crystalline species</li> <li>○ qualitative and quantitative information</li> <li>○ reaction profiles for crystalline species</li> <li>○ contactless, <i>i.e.</i> sample is not disturbed</li> <li>○ direct access to changes in crystal structures</li> <li>○ allows particle size monitoring</li> <li>○ provides data relevant to the body of the sample</li> </ul>	<ul style="list-style-type: none"> <li>○ requires a synchrotron X-ray source</li> <li>○ less informative for amorphous phases</li> </ul>	<ul style="list-style-type: none"> <li>○ crystalline</li> </ul>
Raman	<ul style="list-style-type: none"> <li>○ identification of chemical species and selected functionalities</li> <li>○ sensitive to changes in molecular structure and inter- and intra-molecular interactions</li> <li>○ provides qualitative and quantitative information</li> <li>○ enables extraction of reaction profiles</li> <li>○ can be performed using a laboratory benchtop instrument</li> <li>○ contactless, <i>i.e.</i> sample is not disturbed</li> <li>○ may allow excellent time resolution</li> <li>○ sensitive to isotopes (e.g. H/D exchange)</li> </ul>	<ul style="list-style-type: none"> <li>○ strong luminescence may saturate the Raman signal</li> <li>○ requires translucent milling jars</li> <li>○ sensitivity depends on the Raman signal of individual components</li> <li>○ incident laser beam may induce degradation due to local heating</li> <li>○ signal is obtained mostly from the surface of milled sample</li> </ul>	<ul style="list-style-type: none"> <li>○ crystalline</li> <li>○ amorphous</li> <li>○ liquid</li> </ul>
Temperature	<ul style="list-style-type: none"> <li>○ provides bulk temperature</li> </ul>	<ul style="list-style-type: none"> <li>○ provides bulk temperature</li> </ul>	<ul style="list-style-type: none"> <li>○ any</li> </ul>

monitoring	<ul style="list-style-type: none"> <li>allows modeling of heat transfer</li> </ul>	<ul style="list-style-type: none"> <li>no direct information on the chemical composition</li> <li>requires a thermal sensor in or within the milling vessel</li> </ul>	
Pressure monitoring	<ul style="list-style-type: none"> <li>enables kinetic modeling if gaseous reactants or products are involved</li> </ul>	<ul style="list-style-type: none"> <li>relevant for gaseous reactants or products</li> <li>requires a pressure transducer within the milling vessel</li> </ul>	<ul style="list-style-type: none"> <li>gas</li> </ul>

## Atomic and molecular dynamics of milled solids

Milling is often seen as a methodology for particle comminution and material amorphisation.<sup>44</sup> However, the average particle size in a milled sample will often reach a steady state balancing crystal crushing and growth.<sup>45</sup> To gain insight into such dynamics on the molecular level, we have used isotope-labelled solids to confirm atomic and molecular migrations across the entire milled sample and have effectively shown that the entire sample becomes exposed to the surface during milling.<sup>3</sup> The tandem application of *in situ* Raman spectroscopy and synchrotron PXRD enabled the observation of hydrogen isotope exchange (HIE) between molecules of benzoic acid and 2-pyridone in the course of cocrystal formation. (Figure 4a).

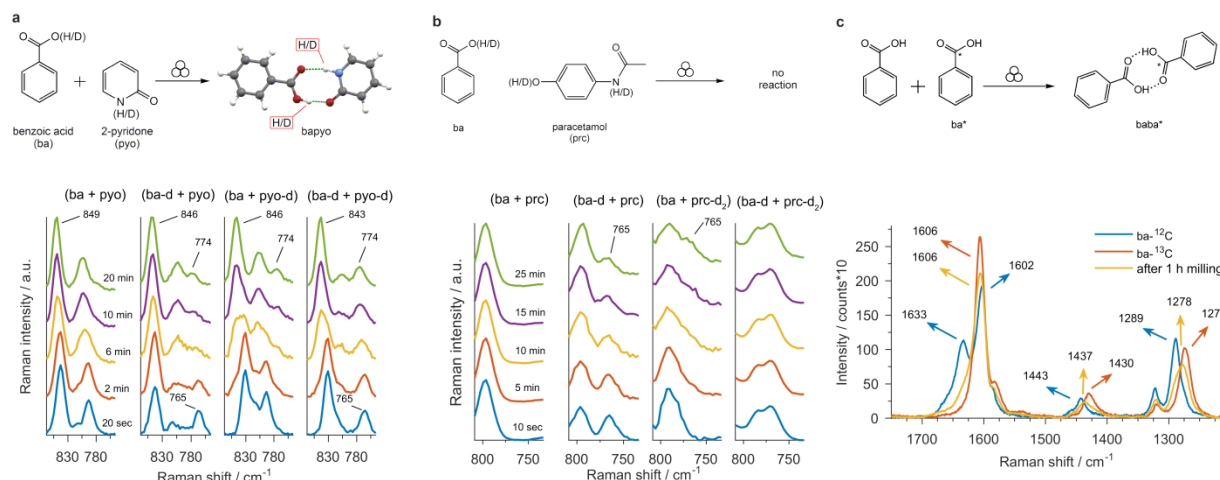


**Figure 4.** Dynamics of milled particles. (a) HIE between benzoic acid and 2-pyridone during cocrystal formation. (b) HIE between milled particles that do not form a new product phase. (c) Molecular exchange between <sup>13</sup>C-labelled benzoic acid and natural benzoic acid leading to the formation of heterodimers.

Since the HIE process was difficult to separate from the formation of the new crystalline product, 2-pyridone was subsequently replaced with paracetamol, which does not form a new crystalline

phase with benzoic acid (Figure 4b).<sup>46</sup> Neat grinding of this mixture, in which one of the two components was deuterated, proved that HIE occurs also between non-reacting solids. Finally, neat grinding of <sup>13</sup>C-labeled benzoic acid and natural benzoic acid resulted in whole-molecule exchange between crystallites and the formation of heterodimers of labelled and natural molecules of benzoic acid (Figure 4c). Considering that the exchange of molecules across the surface of two compressed particles was also demonstrated theoretically,<sup>47</sup> milling of solids seems to share significant resemblance<sup>40,48,49</sup> with solution in terms of atomic and molecular mobility.

## Stepwise reaction mechanisms and intermediates

Assigning a mechanism to a milling reaction typically involves detecting a sequence of crystalline or amorphous phases leading from the reactant(s) to the product(s). If the reaction conditions change, the reaction course may become different, thus offering an insight into the energy profile of such a reaction sequence.<sup>50</sup> The use of *in situ* monitoring is particularly valuable for the detection, and even isolation, of reaction intermediates in mechanochemical reactions, notably for organic and metal-organic systems where such transient phases can readily transform within minutes.

We illustrated the potential of *in situ* monitoring for new phase discovery in the mechanochemical formation of the MOF material ZIF-8, by milling ZnO and 2-methylimidazole (**HMeIm**) in the presence of aqueous acetic acid (Figure 5a-c). While the reaction rapidly produces the target ZIF-8, further milling led to amorphization which was, surprisingly, followed by the appearance of a new crystalline phase. The new phase could be isolated and structurally characterized from PXRD data as a new polymorph of ZIF-8, exhibiting a hitherto unknown katsenite (kat) framework topology.<sup>51</sup> Under mechanochemical conditions, this new polymorph of ZIF-8 would transform after 10-15 minutes to the thermodynamically stable, non-porous framework with the diamondoid (dia) topology. Loss of the diffraction signal upon amorphization renders the use of an internal scattering standard, such as crystalline silicon,<sup>40</sup> essential to extract quantitative reaction profiles – including the weight fraction of the amorphous phase.

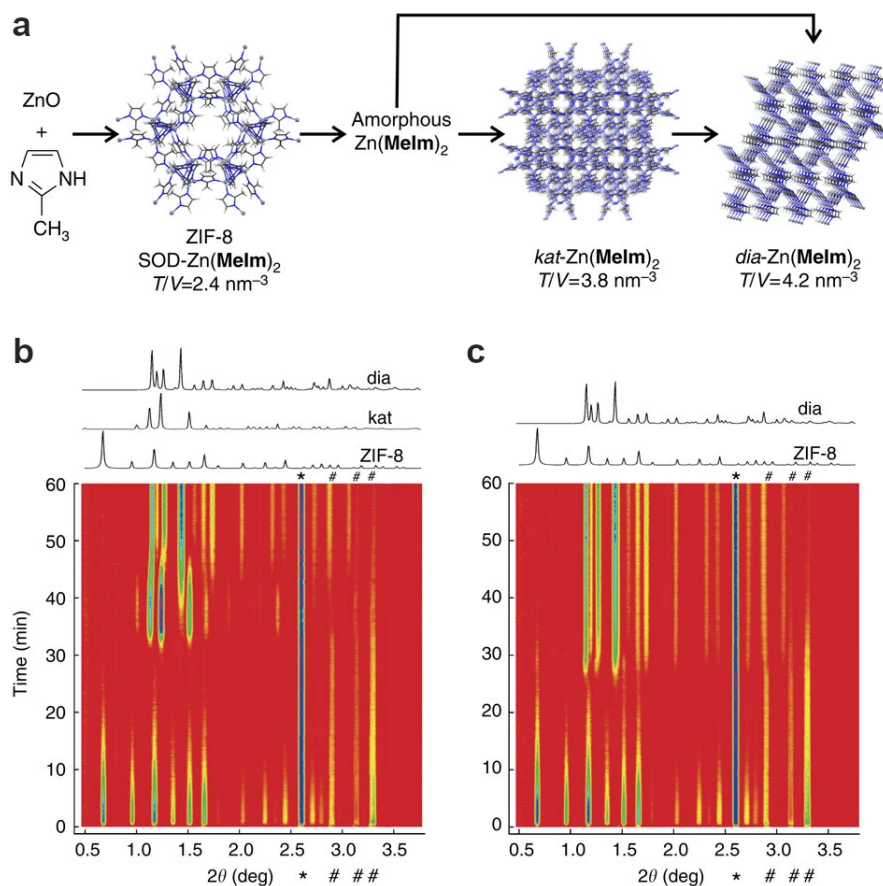


**Figure 5.** (a) Reaction sequence for amorphization of nascent ZIF-8 and recrystallization of the milled mixture into the dense *dia*-topology phase, mediated by a zeolitic imidazolate framework intermediate with a novel katsenite (*kat*) topology. The reflection of silicon used as an internal standard is marked with ‘\*’. Time-resolved diffractograms that demonstrate the stochastic nature of the reaction sequence, with nominally identical experiments showing: (b) the appearance of the *kat*-phase and (c) the absence of the *kat*-phase.

Real-time PXRD monitoring of the liquid-assisted grinding (LAG) reaction of ZnO and 2,5-dihydroxyterephthalic acid (H<sub>4</sub>dhta) in the presence of H<sub>2</sub>O to form the popular open-structure framework Zn-MOF-74 of the composition Zn<sub>2</sub>(dhta) revealed a step-wise mechanism with a close-packed coordination polymer of the composition Zn(H<sub>2</sub>dhta) as a distinct intermediate and two more earlier transient intermediates (Figure 6).<sup>52</sup> In case of ZIFs, their LAG synthesis involves the formation of intermediates that are polymorphs of the final product, while the intermediate in the case of Zn-MOF-74 exhibits a framework composition different from the final product. Recently, *ex situ* PXRD analysis identified a total of four intermediates in LAG mechanosynthesis of MOF-74 from ZnO when using DMF as the liquid additive.<sup>53</sup>

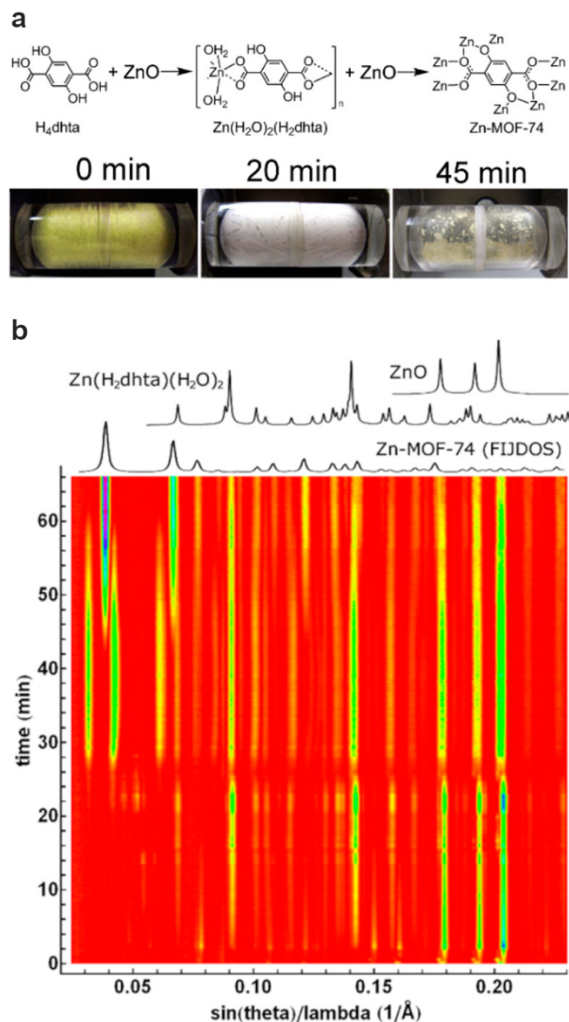


Figure 6. (a) The *in situ* observed sequence of phases for mechanochemical synthesis of Zn-MOF-74 (top) along with selected images of the reaction mixture (bottom) and (b) a time-resolved X-ray diffractogram.

Another example of transient phases detected by real-time *in situ* studies are aryl N-thiocarbamoylbenzotriazoles, elusive intermediates in the well-known Katritzky synthesis of thioureas by thiocarbonylation of amines with bis(benzotriazolyl)methanethione. Specifically, whereas aryl N-thiocarbamoylbenzotriazoles have been proposed as generally occurring reaction intermediates, they have been impossible to isolate due to a high propensity to dissociate into corresponding isothiocyanates.<sup>54</sup> Raman spectroscopy monitoring of the mechanochemical reaction between selected aniline derivatives and bis(benzotriazolyl)methanethione in the 2:1 respective stoichiometric ratio revealed that thiourea formation takes place through a transient intermediate phase. Switching to the 1:1 stoichiometric ratio of reagents enabled the identical intermediates to be isolated as pure phases, and structurally characterized from PXRD data confirmed their identity as elusive aryl N-thiocarbamoylbenzotriazoles (Figure 7a,b).<sup>55</sup>

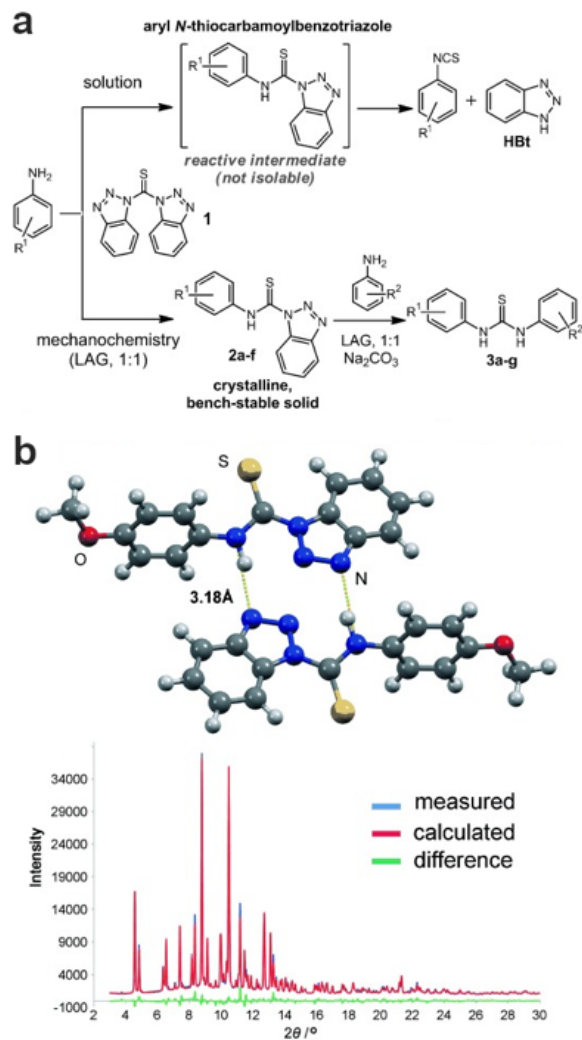


Figure 7. (a) Comparison of thiourea synthesis in solution and by milling. b) Fragment of the crystal structure of the aryl *N*-thiocarbamoylbenzotriazole reaction intermediate determined from PXRD data.<sup>55</sup>

A unique intermediate was observed in the Knoevenagel reaction between vanillin and barbituric acid where the two reactants formed a 1:1 cocrystal prior to the condensation reaction (Figure 8).<sup>42</sup> Through the use of non-protic liquid additives such as nitromethane or acetonitrile, the lifespan of the intermediate cocrystal could be prolonged, while protic liquids led to a faster condensation reaction (Figure 8c). Moreover, the molecules of barbituric acid and vanillin in the intermediate cocrystal were favorably positioned for the nucleophilic attack of barbituric acid at the aldehyde carbon atom of vanillin (Figure 8d).

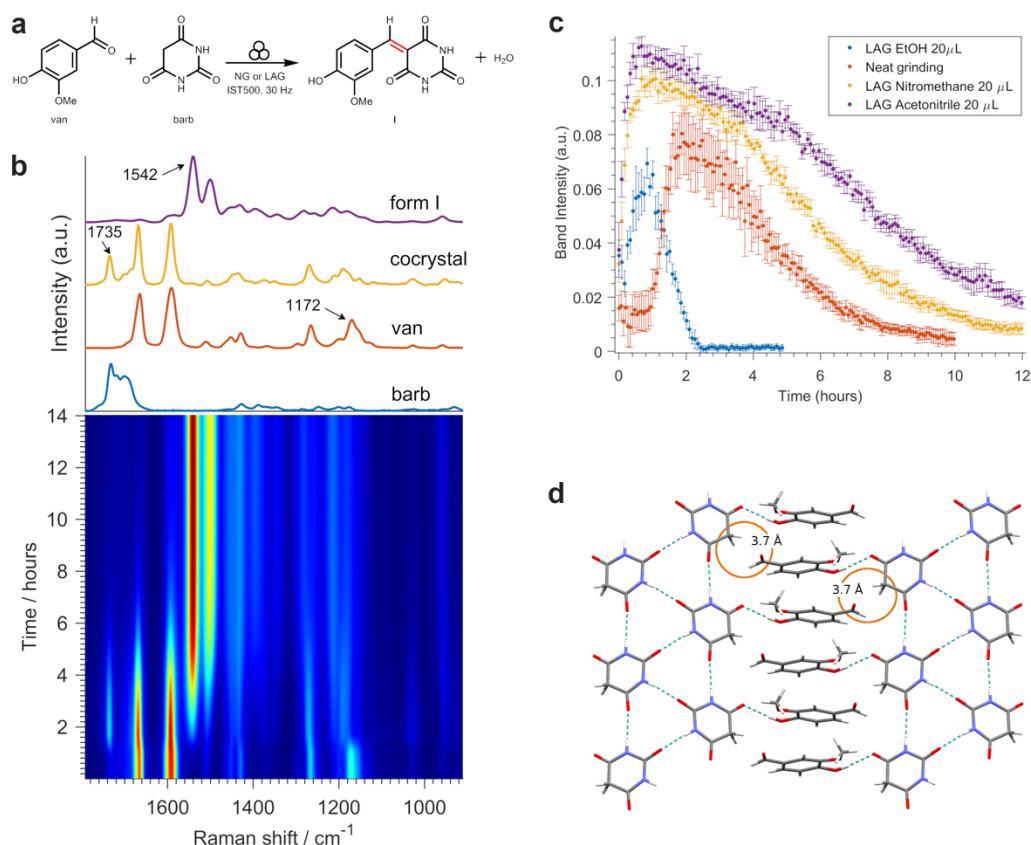


Figure 8. (a) Schematic of the Knoevenagel condensation along with the corresponding (b) time-resolved Raman diffraction data revealing an intermediate (cocystal) evident from the band at 1735  $\text{cm}^{-1}$ . (c) Reaction profiles showing the life-span of the intermediate cocystal in neat grinding and LAG reactions. (d) A fragment of the cocystal structure highlighting proximity of reacting centers.

In our experience, intermediates in mechanochemical reaction are found frequently. Indeed, intermediates and step-wise mechanisms were observed in some of the first *ex situ* step-wise monitoring attempts.<sup>12</sup> The richness of reaction paths involving intermediates can fully be appreciated only through *in situ* monitoring where even short-lived intermediates can be observed.<sup>56</sup> For example, among four polymorphs found in mechanochemical cocystal formation between nicotinamide and benzoic acid,<sup>25</sup> three could be isolated as pure phases, but the fourth polymorph was observed only as fleeting intermediate persisting for a couple of minutes in the very beginning of milling. The plethora of intermediates has inspired exploiting the availability of different solid forms, (e.g. desmotropes, cocystals, salts, polymorphs) as starting reactants to manipulate mechanochemical reaction rates and mechanisms.<sup>57</sup>

## Observation of catalysis and autocatalysis

In mechanochemical reactions, catalysis by milling additives or autocatalysis by a reaction product should be differentiated from similar effects arising from a change in milling conditions

such as milling frequency,<sup>58,59</sup> number and type of milling media,<sup>60,61</sup> and the material of the milling assembly.<sup>4</sup> The latter parameter can be used to adjust the input of mechanical energy at impact,<sup>62,63</sup> affect mixing efficiency, or catalyze coupling reactions.<sup>64</sup> Importantly, the use of milling media with higher density or weight is anticipated to produce a higher steady-state temperature, which can enhance the reaction kinetics.<sup>28</sup> Sometimes, however, an external catalyst is essential to enable a transformation. For example, the milling reaction of  $\text{AgNO}_3$  with sulphadiazine to form the known active pharmaceutical ingredient (API) silver sulphadiazine could not proceed without the presence of aqueous ammonia.<sup>65</sup> However, increasing the amount of ammonia also led to a slower reaction, most likely due to the competing formation of a stabilized silver(I) species.

Liquid additives can have a profound, yet still poorly understood, impact on mechanochemical reactions.<sup>66</sup> A special case of reaction acceleration by a liquid additive arises upon using solvated reactants, where the release of the structural solvent upon a mechanochemical reaction may lead to autocatalysis. Such autocatalytic behavior, so far studied in the mechanochemical formation of cocrystals<sup>67,68</sup> and coordination compounds, offers an explanation for the general observation that solvated starting materials are more reactive than the corresponding non-solvated systems.<sup>69</sup> Our team has reported the *in situ* observation of such autocatalytic behavior as a serendipitous discovery during real-time monitoring of the formation of coordination polymers involving  $\text{CdCl}_2$  and cyanoguanidine (cnge) (Figure 9).<sup>70</sup> Preparation of the reaction mixture in air led to inadvertent partial transformation of the reactant  $\text{CdCl}_2$  to the corresponding monohydrate  $\text{CdCl}_2 \cdot \text{H}_2\text{O}$ . The reaction profile, obtained by quantitative Rietveld analysis, revealed an unexpected difference in the reactivity of metal precursors: while  $\text{CdCl}_2$  was being depleted, the content of  $\text{CdCl}_2 \cdot \text{H}_2\text{O}$  remained largely constant. Once  $\text{CdCl}_2$  was, according to PXRD analysis, fully consumed, the transformation of the  $\text{CdCl}_2 \cdot \text{H}_2\text{O}$  was almost instantaneous. These unusual observations were explained by a reaction loop in which  $\text{CdCl}_2 \cdot \text{H}_2\text{O}$  reacts with cnge, and the released water is immediately captured by anhydrous  $\text{CdCl}_2$  to regenerate the monohydrate. Once  $\text{CdCl}_2$  was fully depleted the released water remained in the mixture leading to autocatalytic reaction acceleration.<sup>70</sup>

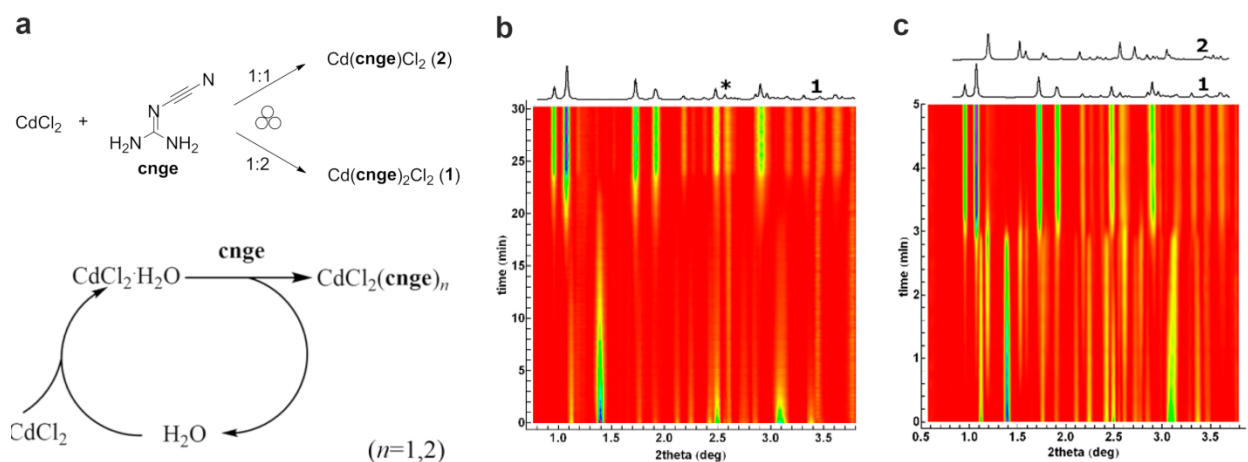


**Figure 9.** (a) The reaction of  $\text{CdCl}_2$  with cyanoguanidine (**cnge**) revealed a feedback mechanism for replenishing  $\text{CdCl}_2 \cdot \text{H}_2\text{O}$ . Time-resolved diffractograms for reactions conducted (b) at room temperature and (c) at  $70^\circ\text{C}$ .

Autocatalytic effect in a mechanochemical reaction was also observed in the formation of the fertilizer ionic cocrystal calcium urea phosphate from urea phosphate and a suitable calcium source, such as  $\text{Ca}(\text{OH})_2$  or  $\text{CaCO}_3$  (calcite) (Figure 10).<sup>71</sup> Reaction monitoring using *in situ* synchrotron PXRD and Raman scattering revealed a slow reaction if starting from neat  $\text{CaCO}_3$ , but which is accelerated by switching to LAG with water. In contrast, the neat reaction with  $\text{Ca}(\text{OH})_2$  as the source of calcium was much faster, which was explained by the release of water during the reaction. This enabled engineering of the reaction rate by using judiciously prepared mixtures of  $\text{CaCO}_3$  and  $\text{Ca}(\text{OH})_2$  as the starting calcium source. While effectively demonstrating how small amounts of  $\text{Ca}(\text{OH})_2$  can be used to facilitate the transformation of  $\text{CaCO}_3$ , this has revealed autocatalysis at water amounts at least three orders of magnitude below those used in typical LAG reaction designs.

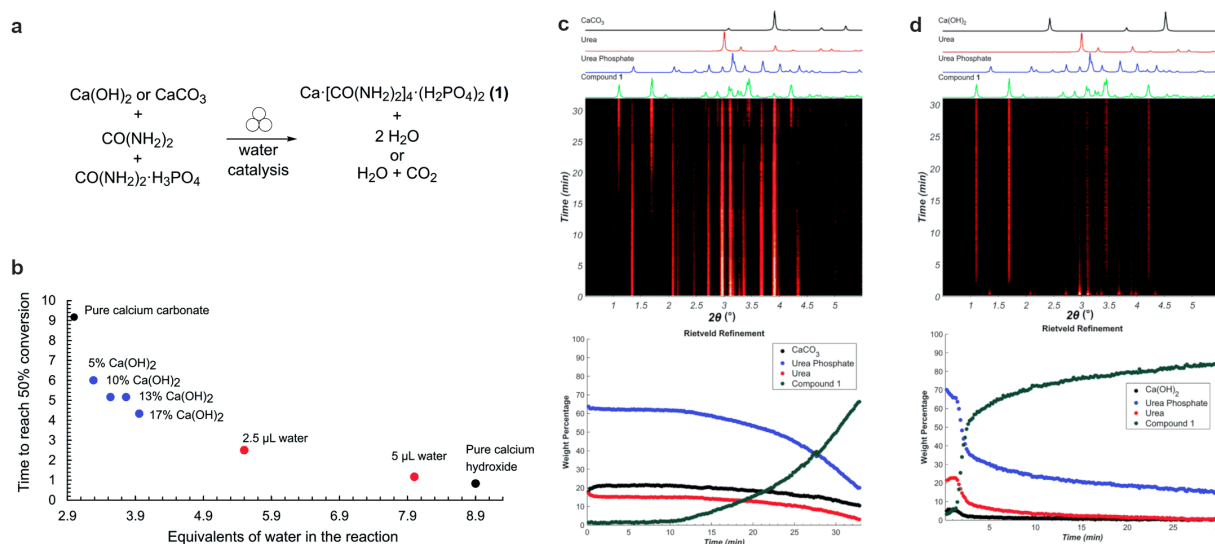


**Figure 10.** Real-time observation of the mechanochemical formation of the ionic cocrystal fertilizer calcium urea phosphate reveals autocatalysis by the water reaction byproduct: (a) reaction scheme; (b) comparison of reaction rates, in the form of time required to reach 50% conversion, for the mechanochemical reactions using neat  $\text{CaCO}_3$ , neat  $\text{Ca}(\text{OH})_2$ , neat mixtures of  $\text{CaCO}_3$  and  $\text{Ca}(\text{OH})_2$ , as well as by LAG of  $\text{CaCO}_3$  in presence of water; (c) and (d) example time-resolved diffractograms (top) and reaction profiles (bottom) for the reactions starting from  $\text{CaCO}_3$  and  $\text{Ca}(\text{OH})_2$ , respectively.

There have been only a handful of examples in which the mechanism of action of a liquid additive was interpreted on a molecular basis. One such example is amide formation by reaction of acyl azides and amines in which the reaction rate was found to increase with basicity of the liquid additive, consistent with deprotonation in the rate-determining step (Figure 11).<sup>72</sup> Mechanochemical synthesis of the archetypal metal-organic framework HKUST-1<sup>73</sup> from copper(II) acetate and trimesic acid demonstrated that the role of the liquid was not only to fill the pores of the nascent HKUST-1, but actively participated in the reaction.<sup>39</sup> In the mechanochemical synthesis of hydrogen-bonding frameworks,<sup>74</sup> as well as covalent-organic frameworks (COFs), the liquid additive templated the formation of the final product network.<sup>75</sup> Catalysis in mechanochemical

reactions is not limited to additives. The material of the milling assembly or the milling media can act as catalysts, as shown for copper-catalyzed azide/alkyne cycloaddition<sup>76</sup> and palladium-catalyzed Suzuki coupling.<sup>77</sup>

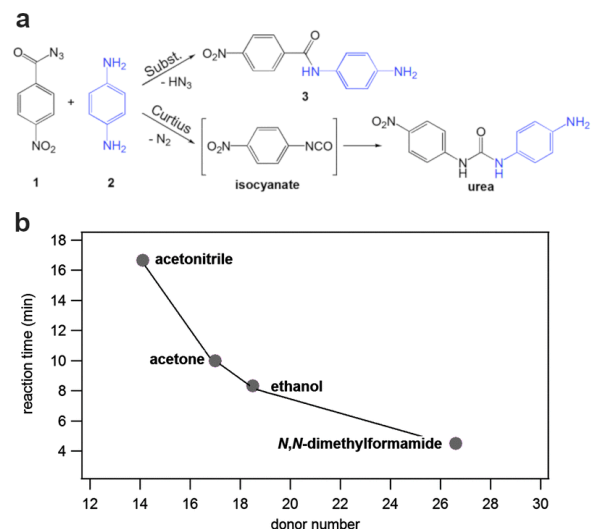


**Figure 11.** A base catalyzes amide bond formation in LAG. (a) New amide bond formation and (b) correlation of the reaction time with basicity of the liquid additive, expressed as the Gutmann donor number.<sup>78</sup>

## Mechanochemical reaction paths, thermodynamics, and selectivity

Mechanochemical reaction paths and the sequence of transformations between cocrystals can be predicted from calculated cocrystal stabilities, as demonstrated so far for hydrogen-bonded<sup>79</sup> and halogen-bonded cocrystals (Figure 12).<sup>80</sup> In the former case, cocrystals of nicotinamide (**na**) with either salicylic acid (**sal**) and anthranilic acid (**ana**) were subjected to milling with the competing cofomer. By using periodic density-functional theory (DFT) calculations, **nasal** was determined to be the most stable cocrystal and, upon milling with **ana**, the mixture composition did not change. However, upon milling with **sal**, **naana** no longer represents the most stable cocrystal and reacts to form **nasal** and solid **ana**. While **sal** displaces **ana** from **naana**, it also reacts with the nascent **ana** to produce the **salana** cocrystal. As **sal** is depleted, the **salana** intermediate becomes the source of **sal** and reacts with remaining **naana**.

With the assumption that mechanochemical cocrystallization leads to the formation of the thermodynamically most stable product, periodic DFT calculations of cocrystal formation energies have been used to correctly predict the direction of mechanochemical transformations of stoichiometric variations of halogen-bonded binary cocrystals consisting of 1,4-diazabicyclo[2.2.2]octane (**dabco**) and 1,2-diiodotetrafluorobenzene (**12tfib**). Specifically, the calculations were used to evaluate changes in crystal energy associated with all possible interconversions of the known cocrystals (**dabco**)(**12tfib**), (**dabco**)<sub>2</sub>(**12tfib**) and (**dabco**)(**12tfib**)<sub>2</sub>. Mechanochemical experiments, conducted after the calculations have been performed, have confirmed the ability of periodic DFT modelling not only to explain, but also to predict the course of mechanochemical cocrystal interconversions.

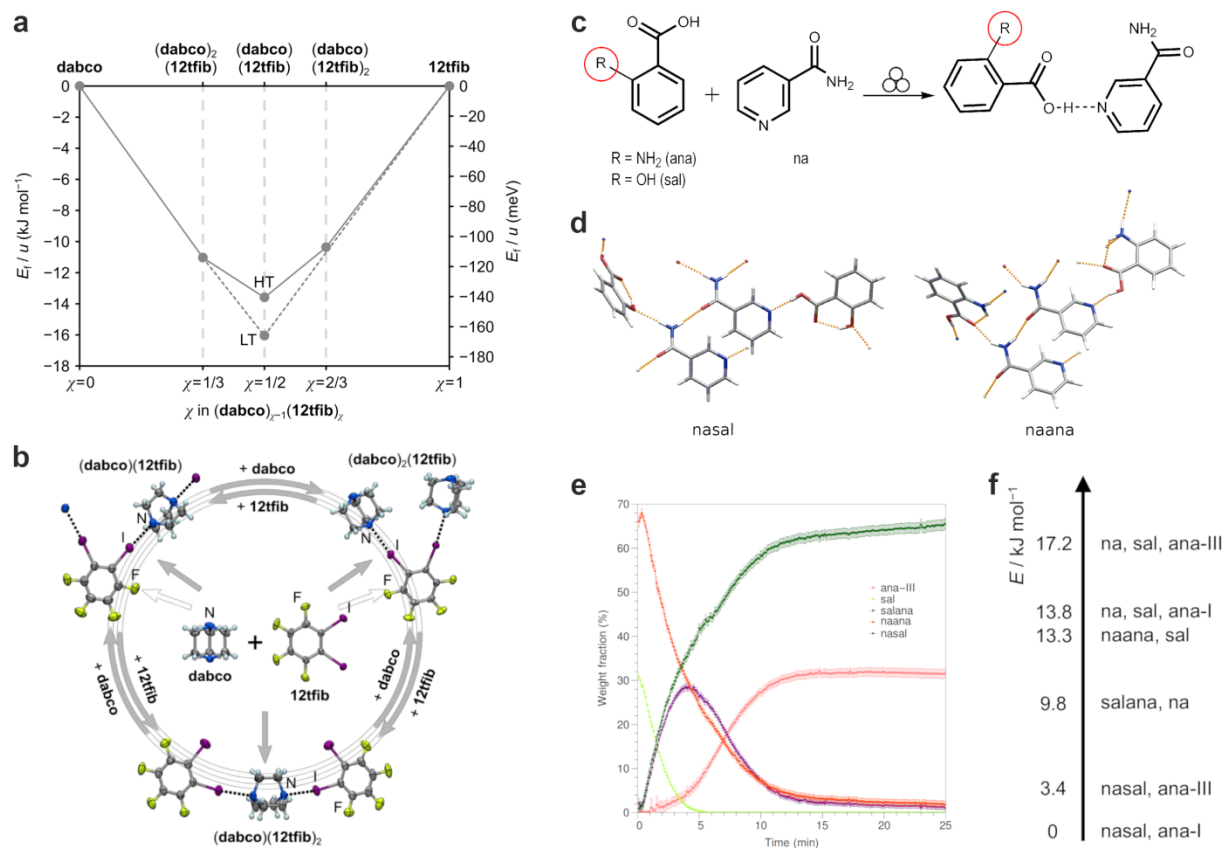


**Figure 12.** Coupling theoretical calculations with mechanochemical cocrystal formation: (a) the theoretically calculated hull diagram indicating the transformations between solid **12tfib**, **dabco** and corresponding cocrystals, along with (b) the corresponding experimentally-observed mechanochemical transformations. c) Cocrystallisation of nicotinamide with anthranilic and salicylic acids and (d) fragments of cocrystal structures. e) Reaction profile for neat grinding of **sal** and **naana** follows (f) the energy ranking of various reaction mixtures.

In the case of cocrystals of **na**, **sal**, and **ana**, the sequence of cocrystal transformations appears to follow the Ostwald's rule of stages, *i.e.* exhibiting the formation of increasingly stable intermediates and, ultimately, the thermodynamically most stable phase. Whereas such behavior is in general agreement with other studies of mechanochemical reactivity conducted *in situ* and *ex situ*,<sup>81</sup> we have also shown that variation of mechanochemical reaction conditions can lead to the formation of products not expected based on the Ostwald's rule. In particular, whereas milling of adipic acid and **na** in PMMA jars typically leads to the thermodynamically stable cocrystal with 1:1 stoichiometry (polymorph I), harsher milling conditions resulted in a metastable polymorph II (Figure 13).<sup>4</sup> The formation of different phases through application of harsher milling conditions was also observed by real-time monitoring of the formation of a

halogen-bonded ionic cocrystal exhibiting either an open network or an interpenetrated Borromean-topology extended structure.<sup>82</sup>

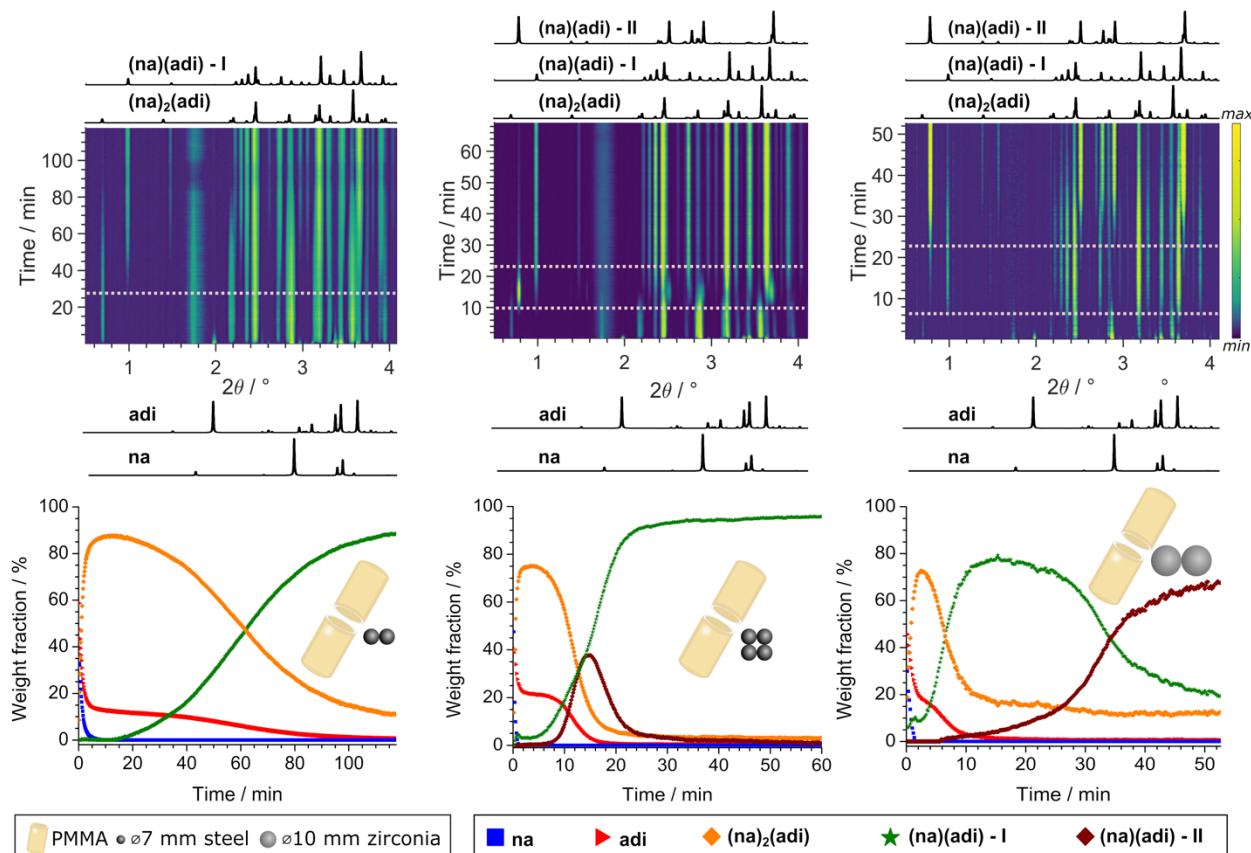
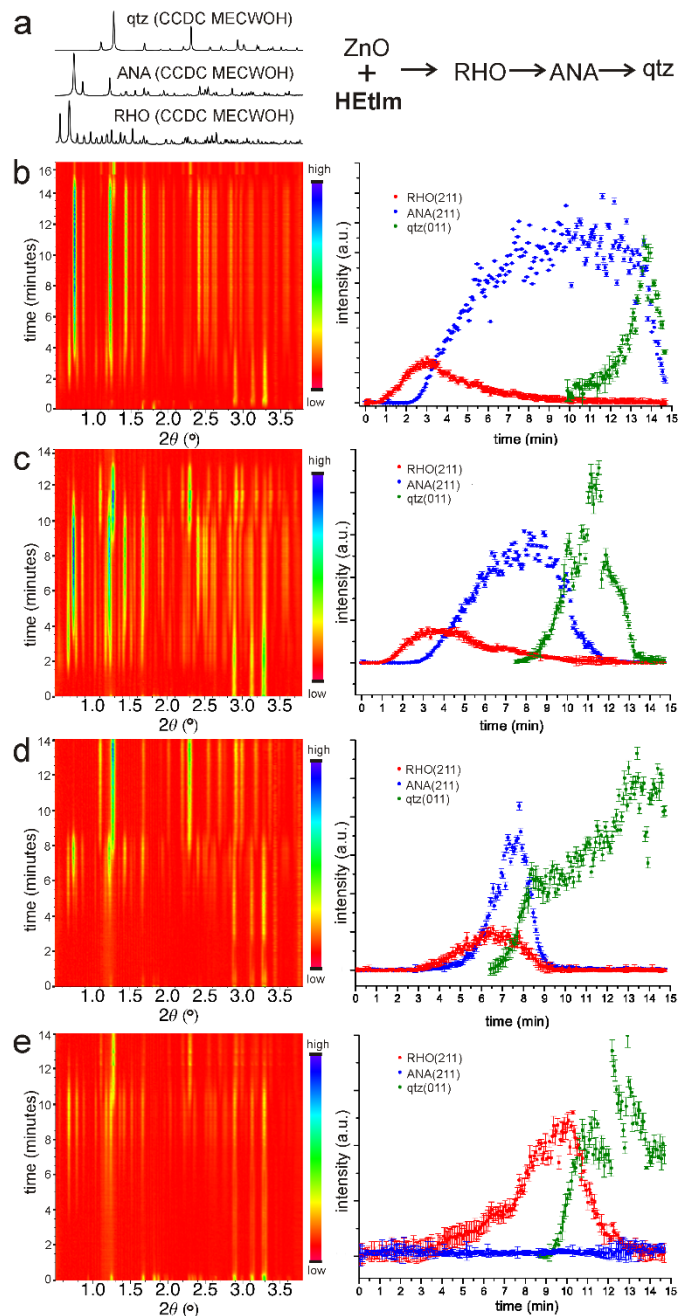


Figure 13. Time-resolved diffractograms and the corresponding reaction profiles for milling of nicotinamide and adipic acid under (from left to right) increasingly harsher milling conditions (illustrated by the number and size of milling balls) eventually leading to a crystallization of the less stable polymorph.

The very first application of synchrotron PXRD for *in situ* reaction monitoring targeted the course of mechanochemical formation of ZIFs from ZnO and substituted imidazoles.<sup>1</sup> Monitoring of the reaction with 2-ethylimidazole in the presence of different amounts of N,N-dimethylformamide (DMF) revealed the initial formation of a low-density framework with the RHO topology, followed by the appearance of increasingly dense frameworks with ANA and qtz topologies. While all reactions ultimately yield the qtz-topology ZIF, the lifetime of the open-structure RHO- and ANA-topology intermediates was longer if more liquid was added, *i.e.* for larger  $\eta$ -values<sup>83</sup> (Figure 14). The combined use of periodic DFT and experimental thermodynamics revealed that this, and other observed reaction sequences in ZIF mechanosynthesis, follow Ostwald's rule of stages.<sup>84</sup>



**Figure 14.** (a) The simulated PXRD patterns and scheme for the reaction of ZnO and HETIm to form the ZIF material Zn(ETIm)<sub>2</sub>. The time-resolved diffractograms (left) and variation of select characteristic Bragg reflections (right) for the mechanochemical transformation of ZnO and HETIm into RHO- (red), ANA- (blue), and qtz-topology (green) polymorphs of Zn(ETIm)<sub>2</sub> by LAG with different amounts of DMF: b) 150  $\mu\text{L}$ ; c) 100  $\mu\text{L}$ ; d) 50  $\mu\text{L}$  and e) 25  $\mu\text{L}$ . The large variation in the intensity of the qtz(011) reflection is an artifact of the sample adhering to the jar wall, caused by the release of the grinding liquid previously included in the pores of intermediates.

Precise temperature monitoring coupled with modeling of heat flow during milling revealed that, in most cases, energy changes related to a chemical reaction will be much smaller compared to thermal effects of friction.<sup>28</sup> The appearance of different materials in the reaction vessel throughout the mechanochemical reaction will lead to different frictional properties of the reaction mixture and, therefore, to a different steady-state temperature resulting from a balance between the absorption of mechanical energy and energy dissipation. Consequently, phase changes taking place during milling, such as polymorphic transformations, can be detected through changes in the steady-state temperature.

Different milling media will not only provide impacts of different energy,<sup>60</sup> but also result in different temperature profiles, which may readily affect the course and rate of mechanochemical reactions. For example, even a mild increase from room temperature to 50 °C can result both in reaction rate acceleration,<sup>70</sup> as well as in a change in reaction path. Such strong influence of temperature suggests that the hot-spot or magma-plasma models<sup>85</sup> of mechanochemical reactivity may not be of relevance for softer organic or metal-organic systems.

## OUTLOOK

We have provided a succinct overview of approaches for real-time monitoring of mechanochemical reactions by ball milling, focusing on contributions from our team. Although significant advances have been achieved in methodologies for real-time observation of such reactivity, we believe these have so far only begun to scratch the surface of understanding, predicting and controlling the course of chemical and materials transformations in a ball mill. Further advances and insights will be enabled through expanding the toolbox on monitoring techniques to approaches different from conventional diffraction and spectroscopy, for example based on nuclear magnetic resonance<sup>21,86</sup> and magnetic relaxation, as well as by closer integration of advanced theoretical approaches with outcomes of real-time measurements.

## BIOGRAPHIES

Stipe Lukin received his M.Sc. and PhD with Ivan Halasz from the University of Zagreb in 2019, working on *in situ* monitoring of mechanochemical reactions, particularly by Raman spectroscopy. His current research focus is on data analysis, *in situ* mechanochemistry, and isotope labeling.

Luzia S. Germann obtained her B.Sc. and M.Sc. from the University of Bern. She completed her PhD at the Max Planck Institute for Solid State Research in Stuttgart under the supervision of Prof. Robert Dinnebier in 2019. She joined the Friščić group in October 2019 to explore mechanochemical formation of cocrystals and molecular functional materials using *in situ* techniques.

Tomislav Friščić earned his B.Sc. in 2001 from the University of Zagreb, under the supervision of Prof. B. Kaitner, and Ph.D. from the University of Iowa, with Prof. L. R. MacGillivray.

Following a post-doctoral stay with Prof. W. Jones at the Pfizer Institute for Pharmaceutical Materials Science and University of Cambridge, he begun independent research as a Herchel Smith Research Fellow, and a Fellow of Sidney Sussex College, University of Cambridge. In 2011 he joined McGill University where he is currently a Professor and Tier-1 Canada Research Chair in Mechanochemistry and Solid-State Reactivity, investigating solid-state reactivity in context of green synthesis and materials.

Ivan Halasz obtained his PhD in 2008 from the University of Zagreb with Prof. Hrvoj Vančik. Following a two-year postdoctoral stint with Prof. Robert Dinnebier at the Max-Planck-Institute for Solid state Research in Stuttgart, he joined as faculty at the Ruđer Bošković Institute in Zagreb. His research focuses on solid-state reactions, mechanochemistry, *in situ* methodology and powder diffraction.

## References

- (1) Friščić, T.; Halasz, I.; Beldon, P. J.; Belenguer, A. M.; Adams, F.; Kimber, S. A. J.; Honkimäki, V.; Dinnebier, R. E. Real-Time and in Situ Monitoring of Mechanochemical Milling Reactions. *Nat. Chem.* **2013**, *5*, 66–73. <https://doi.org/10.1038/nchem.1505>.
- (2) Gracin, D.; Štrukil, V.; Friščić, T.; Halasz, I.; Užarevič, K. Laboratory Real-Time and in Situ Monitoring of Mechanochemical Milling Reactions by Raman Spectroscopy. *Angew. Chem. - Int. Ed.* **2014**, *53*, 6193–6197. <https://doi.org/10.1002/anie.201402334>.
- (3) Lukin, S.; Tireli, M.; Stolar, T.; Barišić, D.; Blanco, M. V.; Di Michiel, M.; Užarevič, K.; Halasz, I. Isotope Labeling Reveals Fast Atomic and Molecular Exchange in Mechanochemical Milling Reactions. *J. Am. Chem. Soc.* **2019**, *141*, 1212–1216. <https://doi.org/10.1021/jacs.8b12149>.
- (4) Germann, L. S.; Arhangelskis, M.; Etter, M.; Dinnebier, R. E.; Friščić, T. Challenging the Ostwald Rule of Stages in Mechanochemical CocrySTALLISATION. *Chem. Sci.* **2020**, *11*, 10092–10100. <https://doi.org/10.1039/D0SC03629C>.
- (5) Do, J.-L.; Friščić, T. Mechanochemistry: A Force of Synthesis. *ACS Cent. Sci.* **2017**, *3*, 13–19. <https://doi.org/10.1021/acscentsci.6b00277>.
- (6) Andersen, J.; Mack, J. Mechanochemistry and Organic Synthesis: From Mystical to Practical. *Green Chem.* **2018**, *20*, 1435–1443. <https://doi.org/10.1039/C7GC03797J>.
- (7) Ardila-Fierro, K. J.; Hernández, J. G. Sustainability Assessment of Mechanochemistry by Using the Twelve Principles of Green Chemistry. *ChemSusChem* **2021**, *14*, 2145–2162. <https://doi.org/10.1002/cssc.202100478>.
- (8) Gomollón-Bel, F. Ten Chemical Innovations That Will Change Our World: IUPAC identifies emerging technologies in Chemistry with potential to make our planet more sustainable. *Chem. Int.* **2019**, *41*, 12–17. <https://doi.org/10.1515/ci-2019-0203>.
- (9) Bowmaker, G. A.; Effendy; Hanna, J. V.; Healy, P. C.; King, S. P.; Pettinari, C.; Skelton, B. W.; White, A. H. Solution and Mechanochemical Syntheses, and Spectroscopic and Structural Studies in the Silver(I) (Bi-)Carbonate: Triphenylphosphine System. *Dalton Trans.* **2011**, *40*, 7210–7218. <https://doi.org/10.1039/C1DT10416K>.
- (10) Štrukil, V.; Fábíán, L.; Reid, D. G.; Duer, M. J.; Jackson, G. J.; Eckert-Maksić, M.; Friščić, T. Towards an Environmentally-Friendly Laboratory: Dimensionality and Reactivity in the Mechanosynthesis of Metal–Organic Compounds. *Chem. Commun.* **2010**, *46*, 9191–9193. <https://doi.org/10.1039/C0CC03822A>.
- (11) Braga, D.; Giuffreda, S. L.; Grepioni, F.; Polito, M. Mechanochemical and Solution Preparation of the Coordination Polymers  $\text{Ag}[\text{N}(\text{CH}_2\text{CH}_2)_3\text{N}]_2[\text{CH}_3\text{COO}]\cdot 5\text{H}_2\text{O}$  and  $\text{Zn}[\text{N}(\text{CH}_2\text{CH}_2)_3\text{N}]\text{Cl}_2$ . *CrystEngComm* **2004**, *6*, 459–462. <https://doi.org/10.1039/B406375A>.

- (12) Cinčić, D.; Friščić, T.; Jones, W. A Stepwise Mechanism for the Mechanochemical Synthesis of Halogen-Bonded Cocrystal Architectures. *J. Am. Chem. Soc.* **2008**, *130*, 7524–7525. <https://doi.org/10.1021/ja801164v>.
- (13) Užarević, K.; Halasz, I.; Friščić, T. Real-Time and in Situ Monitoring of Mechanochemical Reactions: A New Playground for All Chemists. *J. Phys. Chem. Lett.* **2015**, *6*, 4129–4140. <https://doi.org/10.1021/acs.jpcllett.5b01837>.
- (14) Michalchuk, A. A. L.; Emmerling, F. Time-Resolved In Situ Monitoring of Mechanochemical Reactions. *Angew. Chem. Int. Ed. n/a*. <https://doi.org/10.1002/anie.202117270>.
- (15) Vaughan, G. B. M.; Baker, R.; Barret, R.; Bonnefoy, J.; Buslaps, T.; Checchia, S.; Duran, D.; Fihman, F.; Got, P.; Kieffer, J.; Kimber, S. a. J.; Martel, K.; Morawe, C.; Mottin, D.; Papillon, E.; Petitdemange, S.; Vamvakeros, A.; Vieux, J.-P.; Di Michiel, M. ID15A at the ESRF – a Beamline for High Speed Operando X-Ray Diffraction, Diffraction Tomography and Total Scattering. *J. Synchrotron Radiat.* **2020**, *27*, 515–528. <https://doi.org/10.1107/S1600577519016813>.
- (16) Ban, V.; Sadikin, Y.; Lange, M.; Tumanov, N.; Filinchuk, Y.; Černý, R.; Casati, N. Innovative in Situ Ball Mill for X-Ray Diffraction. *Anal. Chem.* **2017**, *89*, 13176–13181. <https://doi.org/10.1021/acs.analchem.7b02871>.
- (17) Lampronti, G. I.; Michalchuk, A. A. L.; Mazzeo, P. P.; Belenguer, A. M.; Sanders, J. K. M.; Bacchi, A.; Emmerling, F. Changing the Game of Time Resolved X-Ray Diffraction on the Mechanochemistry Playground by Downsizing. *Nat. Commun.* **2021**, *12*, 6134. <https://doi.org/10.1038/s41467-021-26264-1>.
- (18) Deidda, C.; Delogu, F.; Cocco, G. In Situ Characterisation of Mechanically-Induced Self-Propagating Reactions. *J. Mater. Sci.* **2004**, *39*, 5315–5318. <https://doi.org/10.1023/B:JMSC.0000039236.48464.8f>.
- (19) Lisac, K.; Topić, F.; Arhangelskis, M.; Cepić, S.; Julien, P. A.; Nickels, C. W.; Morris, A. J.; Friščić, T.; Cinčić, D. Halogen-Bonded Cocrystallization with Phosphorus, Arsenic and Antimony Acceptors. *Nat. Commun.* **2019**, *10*, 61. <https://doi.org/10.1038/s41467-018-07957-6>.
- (20) Julien, P. A.; Arhangelskis, M.; Germann, L. S.; Etter, M.; Dinnebier, R. E.; Morris, A. J.; Friscic, T. Illuminating Mechanochemical Reactions by Combining Real-Time Fluorescence Emission Monitoring and Periodic Time-Dependent Density-Functional Calculations. **2021**. <https://doi.org/10.33774/chemrxiv-2021-lw8sm>.
- (21) Leger, M.; Guo, J.; MacMillan, B.; Titi, H.; Friscic, T.; Blight, B.; Balcom, B. Relaxation Time Correlation NMR for Mechanochemical In-Situ Reaction Monitoring of Metal-Organic Frameworks. **2021**. <https://doi.org/10.33774/chemrxiv-2021-rbj0t>.
- (22) Halasz, I.; Kimber, S. A. J.; Beldon, P. J.; Belenguer, A. M.; Adams, F.; Honkimäki, V.; Nightingale, R. C.; Dinnebier, R. E.; Friščić, T. In Situ and Real-Time Monitoring of Mechanochemical Milling Reactions Using

- Synchrotron X-Ray Diffraction. *Nat. Protoc.* **2013**, *8*, 1718–1729. <https://doi.org/10.1038/nprot.2013.100>.
- (23) Lukin, S.; Užarević, K.; Halasz, I. Raman Spectroscopy for Real-Time and in Situ Monitoring of Mechanochemical Milling Reactions. *Nat. Protoc.* **2021**, 1–40. <https://doi.org/10.1038/s41596-021-00545-x>.
- (24) Batzdorf, L.; Fischer, F.; Wilke, M.; Wenzel, K.-J.; Emmerling, F. Direct In Situ Investigation of Milling Reactions Using Combined X-Ray Diffraction and Raman Spectroscopy. *Angew. Chem. Int. Ed.* **2015**, *54*, 1799–1802. <https://doi.org/10.1002/anie.201409834>.
- (25) Lukin, S.; Stolar, T.; Tireli, M.; Blanco, M. V.; Babić, D.; Friščić, T.; Užarević, K.; Halasz, I. Tandem In Situ Monitoring for Quantitative Assessment of Mechanochemical Reactions Involving Structurally Unknown Phases. *Chem. - Eur. J.* **2017**, *23*, 13941–13949. <https://doi.org/10.1002/chem.201702489>.
- (26) Kulla, H.; Wilke, M.; Fischer, F.; Röllig, M.; Maierhofer, C.; Emmerling, F. Warming up for Mechanochemistry – Temperature Development in Ball Mills during Synthesis. *Chem. Commun.* **2017**, *53*, 1664–1667. <https://doi.org/10.1039/C6CC08950J>.
- (27) Ardila-Fierro, K. J.; Lukin, S.; Etter, M.; Užarević, K.; Halasz, I.; Bolm, C.; Hernández, J. G. Direct Visualization of a Mechanochemically Induced Molecular Rearrangement. *Angew. Chem. - Int. Ed.* **2020**, *59*, 13458–13462. <https://doi.org/10.1002/anie.201914921>.
- (28) Užarević, K.; Ferdelji, N.; Mrla, T.; Julien, P. A.; Halasz, B.; Friščić, T.; Halasz, I. Enthalpy vs. Friction: Heat Flow Modelling of Unexpected Temperature Profiles in Mechanochemistry of Metal-Organic Frameworks. *Chem. Sci.* **2018**, *9*, 2525–2532. <https://doi.org/10.1039/c7sc05312f>.
- (29) Oliveira, P. F. M. de; Michalchuk, A. A. L.; Buzanich, A. G.; Bienert, R.; Torresi, R. M.; Camargo, P. H. C.; Emmerling, F. Tandem X-Ray Absorption Spectroscopy and Scattering for in Situ Time-Resolved Monitoring of Gold Nanoparticle Mechanochemistry. *Chem. Commun.* **2020**, *56*, 10329–10332. <https://doi.org/10.1039/D0CC03862H>.
- (30) Atzmon, M. In Situ Thermal Observation of Explosive Compound-Formation Reaction during Mechanical Alloying. *Phys. Rev. Lett.* **1990**, *64*, 487–490. <https://doi.org/10.1103/PhysRevLett.64.487>.
- (31) Takacs, L. Self-Sustaining Reactions Induced by Ball Milling. *Prog. Mater. Sci.* **2002**, *47*, 355–414. [https://doi.org/10.1016/S0079-6425\(01\)00002-0](https://doi.org/10.1016/S0079-6425(01)00002-0).
- (32) Doppiu, S.; Schultz, L.; Gutfleisch, O. In Situ Pressure and Temperature Monitoring during the Conversion of Mg into MgH<sub>2</sub> by High-Pressure Reactive Ball Milling. *J. Alloys Compd.* **2007**, *427*, 204–208. <https://doi.org/10.1016/j.jallcom.2006.02.045>.
- (33) Chen, Y.; Williams, J. S. Competitive Gas-Solid Reactions Realized by Ball Milling of Zr in Ammonia Gas. *J. Mater. Res.* **1996**, *11*, 1500–1506. <https://doi.org/10.1557/JMR.1996.0187>.

- (34) Troschke, E.; Grätz, S.; Lübken, T.; Borchardt, L. Mechanochemical Friedel-Crafts Alkylation—A Sustainable Pathway Towards Porous Organic Polymers. *Angew. Chem. Int. Ed.* **2017**, *56*, 6859–6863. <https://doi.org/10.1002/anie.201702303>.
- (35) Liu, L.; Lu, L.; Chen, L.; Qin, Y.; Zhang, L. D. Solid-Gas Reactions Driven by Mechanical Alloying of Niobium and Tantalum in Nitrogen. *Metall. Mater. Trans. A* **1999**, *30*, 1097–1100. <https://doi.org/10.1007/s11661-999-0161-2>.
- (36) Bonn, P. van; Bolm, C.; Hernández, J. G. Mechanochemical Palladium-Catalyzed Carbonylative Reactions Using Mo(CO)<sub>6</sub>. *Chem. – Eur. J.* **2020**, *26*, 2576–2580. <https://doi.org/10.1002/chem.201904528>.
- (37) Brekalo, I.; Yuan, W.; Mottillo, C.; Lu, Y.; Zhang, Y.; Casaban, J.; Holman, K. T.; James, S. L.; Duarte, F.; Williams, P. A.; Harris, K. D. M.; Friščić, T. Manometric Real-Time Studies of the Mechanochemical Synthesis of Zeolitic Imidazolate Frameworks. *Chem. Sci.* **2020**, *11*, 2141–2147. <https://doi.org/10.1039/C9SC05514B>.
- (38) Lukin, S.; Stolar, T.; Lončarić, I.; Milanović, I.; Biliškov, N.; Di Michiel, M.; Friščić, T.; Halasz, I. Mechanochemical Metathesis between AgNO<sub>3</sub> and NaX (X = Cl, Br, I) and Ag<sub>2</sub>XNO<sub>3</sub> Double-Salt Formation. *Inorg. Chem.* **2020**, *59*, 12200–12208. <https://doi.org/10.1021/acs.inorgchem.0c01196>.
- (39) Stolar, T.; Batzdorf, L.; Lukin, S.; Žilić, D.; Mottillo, C.; Friščić, T.; Emmerling, F.; Halasz, I.; Užarević, K. In Situ Monitoring of the Mechanosynthesis of the Archetypal Metal-Organic Framework HKUST-1: Effect of Liquid Additives on the Milling Reactivity. *Inorg. Chem.* **2017**, *56*, 6599–6608. <https://doi.org/10.1021/acs.inorgchem.7b00707>.
- (40) Halasz, I.; Friščić, T.; Kimber, S. A. J.; Užarević, K.; Puškarić, A.; Mottillo, C.; Julien, P.; Štrukil, V.; Honkimäki, V.; Dinnebier, R. E. Quantitative in Situ and Real-Time Monitoring of Mechanochemical Reactions. *Faraday Discuss.* **2014**, *170*, 203–221. <https://doi.org/10.1039/c4fd00013g>.
- (41) Germann, L. S.; Katsenis, A. D.; Huskić, I.; Julien, P. A.; Užarević, K.; Etter, M.; Farha, O. K.; Friščić, T.; Dinnebier, R. E. Real-Time in Situ Monitoring of Particle and Structure Evolution in the Mechanochemical Synthesis of UiO-66 Metal-Organic Frameworks. *Cryst. Growth Des.* **2020**, *20*, 49–54. <https://doi.org/10.1021/acs.cgd.9b01477>.
- (42) Lukin, S.; Tireli, M.; Lončarić, I.; Barišić, D.; Šket, P.; Vrsaljko, D.; di Michiel, M.; Plavec, J.; Užarević, K.; Halasz, I. Mechanochemical Carbon-Carbon Bond Formation That Proceeds *via* a Cocrystal Intermediate. *Chem. Commun.* **2018**, *54*, 13216–13219. <https://doi.org/10.1039/C8CC07853J>.
- (43) Bjelopetrović, A.; Lukin, S.; Halasz, I.; Užarević, K.; Đilović, I.; Barišić, D.; Budimir, A.; Juribašić Kulcsár, M.; Čurić, M. Mechanism of Mechanochemical C–H Bond Activation in an Azobenzene Substrate by PdII Catalysts. *Chem. – Eur. J.* **2018**, *24*, 10672–10682. <https://doi.org/10.1002/chem.201802403>.

- (44) Descamps, M.; Willart, J. F. Perspectives on the Amorphisation/Milling Relationship in Pharmaceutical Materials. *Adv. Drug Deliv. Rev.* **2016**, *100*, 51–66. <https://doi.org/10.1016/j.addr.2016.01.011>.
- (45) Mørup, S.; Jiang, J. Z.; Bødker, F.; Horsewell, A. Crystal Growth and the Steady-State Grain Size during High-Energy Ball-Milling. *Europhys. Lett. EPL* **2001**, *56*, 441–446. <https://doi.org/10.1209/epl/i2001-00538-7>.
- (46) Chan, H. C. S.; Kendrick, J.; Neumann, M. A.; Leusen, F. J. J. Towards Ab Initio Screening of Co-Crystal Formation through Lattice Energy Calculations and Crystal Structure Prediction of Nicotinamide, Isonicotinamide, Picolinamide and Paracetamol Multi-Component Crystals. *CrystEngComm* **2013**, *15*, 3799–3807. <https://doi.org/10.1039/C3CE40107C>.
- (47) Ferguson, M.; Moyano, M. S.; Tribello, G. A.; Crawford, D. E.; Bringa, E. M.; James, S. L.; Kohanoff, J.; Pópolo, M. G. D. Insights into Mechanochemical Reactions at the Molecular Level: Simulated Indentations of Aspirin and Meloxicam Crystals. *Chem. Sci.* **2019**, *10*, 2924–2929. <https://doi.org/10.1039/C8SC04971H>.
- (48) Ma, X.; Yuan, W.; Bell, S. E. J.; James, S. L. Better Understanding of Mechanochemical Reactions: Raman Monitoring Reveals Surprisingly Simple ‘Pseudo-Fluid’ Model for a Ball Milling Reaction. *Chem. Commun.* **2014**, *50*, 1585–1587. <https://doi.org/10.1039/C3CC47898J>.
- (49) Pladevall, B. S.; Aguirre, A.; Maseras, F. Understanding Ball Milling Mechanochemical Processes with DFT Calculations and Microkinetic Modeling. *ChemSusChem* **2021**, *14*, 2763–2768. <https://doi.org/10.1002/cssc.202100497>.
- (50) M. Andersen, J.; Mack, J. Decoupling the Arrhenius Equation via Mechanochemistry. *Chem. Sci.* **2017**, *8*, 5447–5453. <https://doi.org/10.1039/C7SC00538E>.
- (51) Katsenis, A. D.; Puškarić, A.; Štrukil, V.; Mottillo, C.; Julien, P. A.; Užarević, K.; Pham, M.-H.; Do, T.-O.; Kimber, S. A. J.; Lazić, P.; Magdysyuk, O.; Dinnebier, R. E.; Halasz, I.; Friščić, T. In Situ X-Ray Diffraction Monitoring of a Mechanochemical Reaction Reveals a Unique Topology Metal-Organic Framework. *Nat. Commun.* **2015**, *6*. <https://doi.org/10.1038/ncomms7662>.
- (52) Julien, P. A.; Užarević, K.; Katsenis, A. D.; Kimber, S. A. J.; Wang, T.; Farha, O. K.; Zhang, Y.; Casaban, J.; Germann, L. S.; Etter, M.; Dinnebier, R. E.; James, S. L.; Halasz, I.; Friščić, T. In Situ Monitoring and Mechanism of the Mechanochemical Formation of a Microporous MOF-74 Framework. *J. Am. Chem. Soc.* **2016**, *138*, 2929–2932. <https://doi.org/10.1021/jacs.5b13038>.
- (53) Beamish-Cook, J.; Shankland, K.; Murray, C. A.; Vaqueiro, P. Insights into the Mechanochemical Synthesis of MOF-74. *Cryst. Growth Des.* **2021**, *21*, 3047–3055. <https://doi.org/10.1021/acs.cgd.1c00213>.
- (54) Katritzky, A. R.; Witek, R. M.; Rodriguez-Garcia, V.; Mohapatra, P. P.; Rogers, J. W.; Cusido, J.; Abdel-Fattah, A. A. A.; Steel, P. J. Benzotriazole-

- Assisted Thioacylation. *J. Org. Chem.* **2005**, *70*, 7866–7881.  
<https://doi.org/10.1021/jo050670t>.
- (55) Štrukil, V.; Gracin, D.; Magdysyuk, O. V.; Dinnebier, R. E.; Friščić, T. Trapping Reactive Intermediates by Mechanochemistry: Elusive Aryl N-Thiocarbamoylbenzotriazoles as Bench-Stable Reagents. *Angew. Chem. - Int. Ed.* **2015**, *54*, 8440–8443. <https://doi.org/10.1002/anie.201502026>.
- (56) Halasz, I.; Puškarič, A.; Kimber, S. A. J.; Beldon, P. J.; Belenguer, A. M.; Adams, F.; Honkimäki, V.; Dinnebier, R. E.; Patel, B.; Jones, W.; Štrukil, V.; Friščić, T. Real-Time in Situ Powder X-Ray Diffraction Monitoring of Mechanochemical Synthesis of Pharmaceutical Cocrystals. *Angew. Chem. - Int. Ed.* **2013**, *52*, 11538–11541.  
<https://doi.org/10.1002/anie.201305928>.
- (57) Kralj, M.; Lukin, S.; Miletić, G.; Halasz, I. Using Desmotropes, Cocrystals, and Salts to Manipulate Reactivity in Mechanochemical Organic Reactions. *J. Org. Chem.* **2021**, *86*, 14160–14168.  
<https://doi.org/10.1021/acs.joc.1c01817>.
- (58) Julien, P. A.; Malvestiti, I.; Friščić, T. The Effect of Milling Frequency on a Mechanochemical Organic Reaction Monitored by in Situ Raman Spectroscopy. *Beilstein J. Org. Chem.* **2017**, *13*, 2160–2168.  
<https://doi.org/10.3762/bjoc.13.216>.
- (59) Casali, L.; Feiler, T.; Heilmann, M.; Braga, D.; Emmerling, F.; Grepioni, F. Too Much Water? Not Enough? In Situ Monitoring of the Mechanochemical Reaction of Copper Salts with Dicyandiamide. *CrystEngComm* **2022**, *24*, 1292–1298.  
<https://doi.org/10.1039/D1CE01670A>.
- (60) Michalchuk, A. A. L.; Tumanov, I. A.; Boldyreva, E. V. Ball Size or Ball Mass – What Matters in Organic Mechanochemical Synthesis? *CrystEngComm* **2019**, *21*, 2174–2179.  
<https://doi.org/10.1039/C8CE02109K>.
- (61) Fischer, F.; Fendel, N.; Greiser, S.; Rademann, K.; Emmerling, F. Impact Is Important—Systematic Investigation of the Influence of Milling Balls in Mechanochemical Reactions. *Org. Process Res. Dev.* **2017**, *21*, 655–659.  
<https://doi.org/10.1021/acs.oprd.6b00435>.
- (62) Carta, M.; Delogu, F.; Porcheddu, A. A Phenomenological Kinetic Equation for Mechanochemical Reactions Involving Highly Deformable Molecular Solids. *Phys. Chem. Chem. Phys. PCCP* **2021**.  
<https://doi.org/10.1039/d1cp01361k>.
- (63) Colacino, E.; Carta, M.; Pia, G.; Porcheddu, A.; Ricci, P. C.; Delogu, F. Processing and Investigation Methods in Mechanochemical Kinetics. *ACS Omega* **2018**, *3*, 9196–9209.  
<https://doi.org/10.1021/acsomega.8b01431>.
- (64) Hwang, S.; Grätz, S.; Borchardt, L. A Guide to Direct Mechanocatalysis. *Chem. Commun.* **2022**. <https://doi.org/10.1039/D1CC05697B>.
- (65) Sović, I.; Lukin, S.; Meštrović, E.; Halasz, I.; Porcheddu, A.; Delogu, F.; Ricci, P. C.; Caron, F.; Perilli, T.; Dogan, A.; Colacino, E. Mechanochemical Preparation of Active Pharmaceutical Ingredients Monitored by *In Situ*

- Raman Spectroscopy. *ACS Omega* **2020**, *5*, 28663–28672.  
<https://doi.org/10.1021/acsomega.0c03756>.
- (66) Shan, N.; Toda, F.; Jones, W. Mechanochemistry and Co-Crystal Formation: Effect of Solvent on Reaction Kinetics. *Chem. Commun.* **2002**, No. 20, 2372–2373. <https://doi.org/10.1039/B207369M>.
- (67) Karki, S.; Friščić, T.; Jones, W.; Motherwell, W. D. S. Screening for Pharmaceutical Cocrystal Hydrates via Neat and Liquid-Assisted Grinding. *Mol. Pharm.* **2007**, *4*, 347–354.  
<https://doi.org/10.1021/mp0700054>.
- (68) Losev, E. A.; Boldyreva, E. V. The Role of a Liquid in “Dry” Co-Grinding: A Case Study of the Effect of Water on Mechanochemical Synthesis in a “L-Serine–Oxalic Acid” System. *CrystEngComm* **2014**, *16*, 3857–3866.  
<https://doi.org/10.1039/C3CE42321B>.
- (69) DeGroot, H. P.; Hanusa, T. P. Solvate-Assisted Grinding: Metal Solvates as Solvent Sources in Mechanochemically Driven Organometallic Reactions. *Organometallics* **2021**, *40*, 3516–3525.  
<https://doi.org/10.1021/acs.organomet.1c00316>.
- (70) Užarević, K.; Štrukil, V.; Mottillo, C.; Julien, P. A.; Puškarić, A.; Friščić, T.; Halasz, I. Exploring the Effect of Temperature on a Mechanochemical Reaction by in Situ Synchrotron Powder X-Ray Diffraction. *Cryst. Growth Des.* **2016**, *16*, 2342–2347. <https://doi.org/10.1021/acs.cgd.6b00137>.
- (71) Julien, P. A.; Germann, L. S.; Titi, H. M.; Etter, M.; Dinnebier, R. E.; Sharma, L.; Baltrusaitis, J.; Friščić, T. In Situ Monitoring of Mechanochemical Synthesis of Calcium Urea Phosphate Fertilizer Cocrystal Reveals Highly Effective Water-Based Autocatalysis. *Chem. Sci.* **2020**, *11*, 2350–2355. <https://doi.org/10.1039/C9SC06224F>.
- (72) Tireli, M.; Juribašić Kulcsár, M.; Cindro, N.; Gracin, D.; Biliškov, N.; Borovina, M.; Ćurić, M.; Halasz, I.; Užarević, K. Mechanochemical Reactions Studied by in Situ Raman Spectroscopy: Base Catalysis in Liquid-Assisted Grinding. *Chem. Commun.* **2015**, *51*, 8058–8061.  
<https://doi.org/10.1039/C5CC01915J>.
- (73) Chui, S. S.-Y.; Lo, S. M.-F.; Charmant, J. P. H.; Orpen, A. G.; Williams, I. D. A Chemically Functionalizable Nanoporous Material [Cu<sub>3</sub>(TMA)<sub>2</sub>(H<sub>2</sub>O)<sub>3</sub>]<sub>n</sub>. *Science* **1999**.
- (74) Friščić, T.; Trask, A. V.; Motherwell, W. D. S.; Jones, W. Guest-Directed Assembly of Caffeine and Succinic Acid into Topologically Different Heteromolecular Host Networks upon Grinding. *Cryst. Growth Des.* **2008**, *8*, 1605–1609. <https://doi.org/10.1021/cg700929e>.
- (75) Emmerling, S. T.; Germann, L. S.; Julien, P. A.; Moudrakovski, I.; Etter, M.; Friščić, T.; Dinnebier, R. E.; Lotsch, B. V. In Situ Monitoring of Mechanochemical Covalent Organic Framework Formation Reveals Templating Effect of Liquid Additive. *Chem* **2021**, *7*, 1639–1652.  
<https://doi.org/10.1016/j.chempr.2021.04.012>.
- (76) Cook, T. L.; Walker, J. A.; Mack, J. Scratching the Catalytic Surface of Mechanochemistry: A Multi-Component CuAAC Reaction Using a Copper

- Reaction Vial. *Green Chem.* **2013**, *15*, 617–619.  
<https://doi.org/10.1039/C3GC36720G>.
- (77) Vogt, C. G.; Grätz, S.; Lukin, S.; Halasz, I.; Etter, M.; Evans, J. D.; Borchardt, L. Direct Mechano catalysis: Palladium as Milling Media and Catalyst in the Mechanochemical Suzuki Polymerization. *Angew. Chem. Int. Ed.* **2019**, *58*, 18942–18947.  
<https://doi.org/10.1002/anie.201911356>.
- (78) Gutmann, V. Solvent Effects on the Reactivities of Organometallic Compounds. *Coord. Chem. Rev.* **1976**, *18*, 225–255.  
[https://doi.org/10.1016/S0010-8545\(00\)82045-7](https://doi.org/10.1016/S0010-8545(00)82045-7).
- (79) Lukin, S.; Lončarić, I.; Tireli, M.; Stolar, T.; Blanco, M. V.; Lazić, P.; Užarević, K.; Halasz, I. Experimental and Theoretical Study of Selectivity in Mechanochemical Cocrystallization of Nicotinamide with Anthranilic and Salicylic Acid. *Cryst. Growth Des.* **2018**, *18*, 1539–1547.  
<https://doi.org/10.1021/acs.cgd.7b01512>.
- (80) Arhangel'skis, M.; Topić, F.; Hindle, P.; Tran, R.; Morris, A. J.; Cinčić, D.; Friščić, T. Mechanochemical Reactions of Cocrystals: Comparing Theory with Experiment in the Making and Breaking of Halogen Bonds in the Solid State. *Chem. Commun.* **2020**, *56*, 8293–8296.  
<https://doi.org/10.1039/D0CC02935A>.
- (81) Caira, M. R.; Nassimbeni, L. R.; Wildervanck, A. F. Selective Formation of Hydrogen Bonded Cocrystals between a Sulfonamide and Aromatic Carboxylic Acids in the Solid State. *J. Chem. Soc. Perkin Trans. 2* **1995**, No. 12, 2213–2216. <https://doi.org/10.1039/P29950002213>.
- (82) Catalano, L.; Germann, L. S.; Julien, P. A.; Arhangel'skis, M.; Halasz, I.; Užarević, K.; Etter, M.; Dinnebier, R. E.; Ursini, M.; Cametti, M.; Martí-Rujas, J.; Friščić, T.; Metrangolo, P.; Resnati, G.; Terraneo, G. Open versus Interpenetrated: Switchable Supramolecular Trajectories in Mechano synthesis of a Halogen-Bonded Borromean Network. *Chem* **2021**, *7*, 146–154. <https://doi.org/10.1016/j.chempr.2020.10.022>.
- (83) Friščić, T.; Childs, S. L.; Rizvi, S. A. A.; Jones, W. The Role of Solvent in Mechanochemical and Sonochemical Cocrystal Formation: A Solubility-Based Approach for Predicting Cocrystallisation Outcome. *CrystEngComm* **2009**, *11*, 418–426. <https://doi.org/10.1039/B815174A>.
- (84) Akimbekov, Z.; Katsenis, A. D.; Nagabhushana, G. P.; Ayoub, G.; Arhangel'skis, M.; Morris, A. J.; Friščić, T.; Navrotsky, A. Experimental and Theoretical Evaluation of the Stability of True MOF Polymorphs Explains Their Mechanochemical Interconversions. *J. Am. Chem. Soc.* **2017**, *139*, 7952–7957. <https://doi.org/10.1021/jacs.7b03144>.
- (85) Thiessen, P. A.; Meyer, K.; Heinicke, G. *Grundlagen Der Tribochemie*; Akademie Verlag, Berlin, 1967.
- (86) Schiffmann, J. G.; Emmerling, F.; Martins, I. C. B.; Van Wüllen, L. In-Situ Reaction Monitoring of a Mechanochemical Ball Mill Reaction with Solid State NMR. *Solid State Nucl. Magn. Reson.* **2020**, *109*, 101687.  
<https://doi.org/10.1016/j.ssnmr.2020.101687>.